Mathematisches Forschungsinstitut Oberwolfach

Report No. 58/2007

Material Theories

Organised by
Antonio DeSimone, Trieste
Stephan Luckhaus, Leipzig
Lev Truskinovsky, Palaiseau

December 16th – December 22nd, 2007

Abstract. The workshop reviewed classical and recent trends in the modeling of material behavior using a wide spectrum of mathematical tools (stochastic processes, calculus of variations, pde's). Among the topic covered, the following figured prominently: biology and biophysics, mechanics of nanostuctures, crystal plasticity, self-organized criticality, non equilibrium statistical mechanics, quantum mechanics, wetting phenomena, electronic transport in semiconductors, dislocation mechanics, kinetic theory, bucking in structural mechanics.

Mathematics Subject Classification (2000): 35xx, 49xx, 60Gxx, 74xx, 74A25, 74Cxx, 74Nxx, 74Rxx, 76xx, 82xx, 92C17, 92C37,

Introduction by the Organisers

Physical Sciences and, in particular, Mechanics, have always played an important role as a source of inspiration for Mathematics. They have suggested fundamental problems, and stimulated the development of new techniques and tools. Now it is a particularly exciting time for the interaction of Mathematics and Mechanics: experimental developments in Mechanics and Biophysics at nano scales are posing challenging questions and giving new opportunities to Mathematics.

This became very clear at this meeting. A broad spectrum of problems from such diverse fields of applications as biology and biophysics, mechanics of nanostructures, and crystal plasticity was presented.

From theoretical physics, recent concepts and paradigms such as self-organized criticality, and non equilibrium statistical mechanics as applied to living systems were discussed.

Stochastic processes, calculus of variations, and pde's, up to the theory of Boltzmann equation are the mathematical foundations of the recent results presented at the workshop.

A new topic of attention with respect to the glorious tradition of this conference series was the attempt to establish the foundations of engineering theories at the mesoscopic scales from ab-initio calculations (quantum mechanics).

An important aspect of the meeting was also the contribution from experimentalists, from wetting and contact angle hysteresis phenomena, to intermittency in plasticity, to electronic transport in semiconductors.

The success of the workshop was mostly due to the strong interaction among participants, bridging different fields of expertise, particularly in the discussion on classical fields such as dislocation mechanics, plasticity, kinetic theory and even buckling phenomena in structural mechanics. We have witnessed that several participants were coming out of the meeting with new ideas and new research projects to pursue. Many expressed their appreciation for the open-minded spirit with which problems were presented, and for the constructive spirit of the discussions. The atmosphere at the Institute certainly contributed in a decisive way to the success of the Workshop.

Antonio DeSimone, Stephan Luckhaus, and Lev Truskinovsky

Workshop: Material Theories

Table of Contents

Abstracts

Viscometry of nanostructures

Richard D. James

Perhaps the most important flows studied in fluid mechanics are viscometric flows, while the most important deformations for solids are those describing the bending and twisting of beams. The former are the flows used to measure the viscosities of fluids, and, in the important case of non-Newtonian fluids, they are used to measure normal stress differences. In the case of solids, the bending and twisting of beams, represented most primitively by the St. Venant solutions of linear elasticity, are the basic solutions used to measure the elastic constants.

The purpose of this research is to give a precise atomic level analog of these deformations. In essence, it is seen that all of these solutions have a common atomistic foundation as solutions of the equations of molecular dynamics corresponding to invariant manifolds of these equations. These results are substantially independent of the nature of the atomic forces: it is only assumed that the atomic forces are consistent with the formula for the force on an atom given by, say, the Hellmann-Feynman formula based on Born-Oppenheimer quantum mechanics. These solutions extend to regimes not contemplated by the continuum theories of elasticity and fluid dynamics. For example, they can be used to simulate the bending and twisting of carbon nanotubes with a bending radius on the order of atomic spacing. Some examples of this type are given in [1]. They also suggest interesting atomic level analogs of the viscometric flows of fluids: for example, one can extend a carbon nanotube at constant strain rate. Literally, one can "flow the nanotube" and measure from the simulation an analog of extensional viscosity. All solutions discussed are exact solutions of the equations of molecular dynamics under mild hypotheses: no approximations are made.

The analysis begins with the specification of isometry groups. These are finite or infinite groups consisting of orthogonal transformations and translations, $g \in G$ of the form $g = (Q|c), Q \in \mathrm{SO}(3)$, $c \in R^3$. If $g_1 = (Q_1|c_1)$ and $g_2 = (Q_2|c_2)$ then the product is $g_1 g_2 = (Q_1 Q_2 | Q_1 c_2 + c_1)$, which corresponds to composition of mappings of the form $g(x) = Qx + c$. These form isometry groups, and it is a classical exercise to write down all such discrete groups. Those that contain three linearly independent vectors are called the *space groups*, but the most interesting are perhaps the ones without full periodicity. These were derived by descending from space groups, and, as such, are given as abstract groups, i.e., labeled by symbols that uniquely determine their multiplication tables. For the present application we need the actual elements (the Qs and cs) rather than just the multiplication tables. Also, the most convenient source for these are the International Tables of Crystallography (volume E for the subperiodic groups), but, in fact, these tables are not comprehensive: some groups are missing. For these reasons we have rederived all of these groups in explicit forms (i.e., formulas for the Qs and cs for each group), see [2].

Using the invariance of the expression for the forces under orthogonal transformations and translations, and its invariance under permutations of atoms of like species, one easily justifies the following results. Given a discrete group $G = \{g_1 = id, \dots, g_N\}$ (N can be infinite) of isometries, we assign initial positions $x_{1,1}(0), \dots, x_{1,M}(0)$ and velocities $\dot{x}_{1,1}(0), \dots, \dot{x}_{1,M}(0)$ of a finite number of M of atoms, we solve the M equations

(1)
$$m_j \ddot{x}_{1,j} = -\frac{\partial \varphi(g_1(x_{1,1}(t)), \dots, g_1(x_{1,M}(t)), \dots, g_N(x_{1,1}(t)), \dots, g_N(x_{1,M}(t)))}{\partial x_{1,j}}.$$

subject to the initial positions and velocities given above.

Now define $x_{i,j}(t) = g_i(x_{1,j}(t), i = 1, \dots, N,\ j = 1, \dots, M,\ t > 0$. The basic theorem is that $x_{i,j}(t)$ also satisfy the equations of molecular dynamics. This justifies the following method of simulation: simulate $x_{1,1}(t), \dots, x_{1,M}(t)$ using the equations of molecular dynamics, computing forces from all the atoms. Impose that all other atoms adopt positions given by $\{g_i(x_{1,j}(t) : i = 1, \dots, N, g_i \in G\}$. The proof involves a simple substitution of these positions into the equations of molecular dynamics and a verification that they are satisfied.

One can notice from this proof that in fact, certain time dependencies of the group elements themselves are allowed, preserving the basic theorem. The most general generically-allowed time dependence is that the translational part of the group elements has to be affine in time. These collections of time-dependent isometries still have to form groups, so this leads to an extension of the theorem mentioned earlier: find all discrete groups of isometries whose elements have affine dependence on time. This is given in [2]. One example mentioned above is the extension of a carbon nanotube at constant strain rate.

Another example relies on the translation group $\{g_\nu = (I|(I + tA)\nu^i e_i) : \nu^1, \nu^2, \nu^3 \in Z\}$, where A is a linear transformation on R^3 and e_1, e_2, e_3 are linearly independent vectors in R^3. This gives rise to solutions that include Couette flow of fluid mechanics (take $A = a \otimes n$, $a \cdot n = 0$). To compare with continuum mechanics, one can take $\nu^i e_i \sim x$, so that in Lagrangian form these deformations are represented at macroscopic level by $y(x,t) = (I + At)x$. These have Eulerian velocity $v(y,t) = A(I + At)^{-1}y$. If the constitutive relation for the stress σ has the property that for purely time dependent velocity gradients (for all past time) we have $\operatorname{div} \sigma = 0$, it follows by elementary calculations that the equations of motion $\rho(v_t + \nabla v v) = \operatorname{div} \sigma$ are identically satisfied. This is why these flows are significant in fluid mechanics: no matter what the fluid, these are possible motions. By measuring the traction at the boundary corresponding to various A one can determine directly properties of the constitutive relation, i.e., viscosities and normal stress differences.

How representative are these solutions of the equations of molecular dynamics? That is a key question that may be best approached by methods of nonlinear dynamics. One may conjecture that if one does a sufficient number of simulations using a sequence of larger and larger fundamental domains and corresponding smaller and smaller subgroups, then one approximates in some average sense a

generic solution of the equations of molecular dynamics with suitably restricted initial conditions. Another possible way to understand these solutions is to look at their counterparts in other theories of physics. Considering the example mentioned in the preceding paragraph, we note that, using the heuristic language given above,

- $\dot{x}_{1,j}(t)$ are the velocities of atoms at 0.
- $\dot{x}_{1,j}(t) + A(I + tA)^{-1}y$ are the velocities of atoms at $y = (I + At)x$.
- Hence, the probability of finding an atom with velocity v at position 0 at time t equals the probability of finding an atom with velocity $v + A(I + tA)^{-1}y$ at position y at time t.

Thus, if we think in terms of a molecular density function $f(t, y, v)$, $f : R \times R^3 \times R^3 \to R^{\geq}$, giving the probability of finding an atom with velocity v at t, y, we are led to make the ansatz

$$f(t, y, v + A(I + tA)^{-1}y) = f(t, 0, v). \tag{2}$$

Substituting this ansatz into the Boltzmann equation, a quick calculation shows that it reduces that equation: $f(t, y, v) = g(t, v - A(I + At)^{-1}y)$ gives the following equation for $g(t, w)$,

$$g_t + g_w \cdot A(I + At)^{-1}w = C[g], \tag{3}$$

where C represents the usual collisions operator. Apparently, Truesdell's solution [3] for the infinite set of moment equations in the simple shearing case follows by taking moments of a g solving this equation. His solution has an interesting feature. There is a transient part and a dominant part. The latter is of primary importance. The dominant part apparently would be obtained by looking at the long time limit of (3). It would be extremely interesting to find this limiting equation, as it may give important information on the distribution of velocities in highly nonequilibrium situations.

This report of ongoing work benefited from valuable discussions with Stefan Müller, Traian Dumritica, Satish Kumar and Kaushik Dayal.

References

[1] Traian Dumritica and R. D. James, Objective molecular dynamics, *J. Mechanics and Physics of Solids* **55**, pp. 2206-2236.

[2] Kaushik Dayal, Ryan Elliott and Richard D. James, *Formulas for objective structures*, preprint.

[3] C. Truesdell and R. G. Muncaster, Fundamentals of Maxwell's kinetic theory of a simple monatomic gas, treated as a branch of rational mechanics. Academic Press (1980). See Part D.

The use of Γ-convergence in the analysis of problems with multiple scales

Andrea Braides
(joint work with Lev Truskinovsky)

The notion of Γ-convergence of energies (see [5, 2, 3]) is designed to guarantee the convergence of minimum problems; i.e.,

$$F_\varepsilon \xrightarrow{\Gamma} F^{(0)} \qquad \Longrightarrow \qquad m_\varepsilon := \min F_\varepsilon \to m^{(0)} := \min F^{(0)}, \tag{1}$$

and (almost) minimizers of $\min F_\varepsilon$ converge to minimizers of $F^{(0)}$. This property implies that sometimes the study of complex minimum problems involving a (small) parameter ε can be approximated by a minimum problem where the dependence on this parameter has been averaged out. This implication is valid if some equi-coerciveness assumptions on F_ε are satisfied (i.e., if we may find converging minimizing sequences); throughout this paper we tacitly suppose that such assumptions hold. Moreover, in order not to make the extraction of a Γ-converging sequence a loss of generality, we will tacitly assume that our Γ-limits are computed with respect to a separable metrizable convergence (which is usually the case).

In various cases the computation of the Γ-limit suggests the use of a specific simplified theory for a complex problem depending on ε. This general paradigm may be in contrast with the use of other theories by practitioners, or may provide a poor approximation of the original functional in certain regimes. Our goal is to develop a vocabulary in the direction of overcoming this apparent drawback in the use of Γ-convergence. The proof of the results of this paper can be found in [4] together with various examples.

Parameterized functionals. Minimum problems are often parametrized by 'lower-order terms', whose form does not greatly affect the Γ-limit, being either continuous perturbations or in some way 'compatible' with Γ-convergence (this often is the case for boundary conditions or volume constraints). However, the overall dependence of the limit process on these parameters may be inaccurately described by the Γ-limit.

Singular points. Let F_ε^λ be a family of parametrized functionals, with $\lambda \in \Lambda$. We say that λ_0 is a *singular point* if there exist m_ε, $\lambda'_\varepsilon \to \lambda_0$ and $\lambda''_\varepsilon \to \lambda_0$ such that (up to subsequences)

$$\Gamma\text{-}\lim_{\varepsilon\to 0} (F_\varepsilon^{\lambda'_\varepsilon} - m_\varepsilon) \neq \Gamma\text{-}\lim_{\varepsilon\to 0} (F_\varepsilon^{\lambda''_\varepsilon} - m_\varepsilon), \tag{2}$$

and one of the two limits is not trivial. If λ_0 is not a singular point, we say that it is a *regular point*. We then have the following result, which states that for regular points the Γ-limit procedure provides a uniform approximation of minimum problems.

Theorem (uniform convergence of minimum problems) *If Λ is compact and is composed of regular points, and if $m_\varepsilon(\lambda)$ exist such that the limit*

$$\Gamma\text{-}\lim_{\varepsilon\to 0} F_\varepsilon^\lambda =: F_\lambda^{(0)}$$

exists and is not trivial, then we have

$$\sup_{\Lambda}\left|\min F_\varepsilon^\lambda - \min F_\lambda^{(0)}\right| = o(1).$$

Remark (A necessary condition for regularity) $\lambda \mapsto \min F_\lambda^{(0)}$ is continuous at regular λ_0.

Uniformly-equivalent functionals. A first observation is that equality of Γ-limits gives an equivalence relation between families of energies; i.e., if $\Gamma\text{-}\lim F_\varepsilon = \Gamma\text{-}\lim G_\varepsilon$ then we say that F_ε is equivalent to G_ε. In this way the concept of Γ-limit is substituted by that of its equivalence class; note that the domain of F_ε and G_ε may be completely different. This concept actually needs a more general definition.

We say that two families of parametrized functionals F_ε^λ and G_ε^λ are *uniformly equivalent at* λ_0 if for every sequences $(\varepsilon_j, \lambda_j)$ converging to $(0, \lambda_0)$ such that there exist m_j such that the limits

$$\Gamma\text{-}\lim_j (F_{\varepsilon_j}^{\lambda_j} - m_j), \qquad \Gamma\text{-}\lim_j (G_{\varepsilon_j}^{\lambda_j} - m_j) \tag{3}$$

exists, these are not trivial and are equal.

Theorem. *Let Λ be compact, and let F_ε^λ and G_ε^λ be uniformly equivalent at all $\lambda \in \Lambda$. Then we have*

$$\sup_{\Lambda}\left|\min F_\varepsilon^\lambda - \min G_\varepsilon^\lambda\right| = o(1). \tag{4}$$

At a singular point λ_0 the computation of the Γ-limit with fixed λ_0 is not sufficient to accurately describe the behavior of minimum problems. We have then to look at the different limits that we may obtain as $\lambda_\varepsilon \to \lambda_0$.

Table of Γ-limits at λ_0. The *table of Γ-limits* for F_ε^λ at λ_0 are all sequences $(\varepsilon_j, \lambda_j)$, and functionals $F_{(\varepsilon_j,\lambda_j)}^{(0)}$ with $\varepsilon_j \to 0$, $\lambda_j \to \lambda_0$, and

$$F_{(\varepsilon_j,\lambda_j)}^{(0)} = \Gamma\text{-}\lim_j F_{\varepsilon_j}^{\lambda_j}.$$

The behavior of parametrized energies at a singular point may be sometimes analyzed in terms of curves in the $\varepsilon - \lambda$ space, along which a regular Γ-development exists. This is not the general case, but it is frequent in applications.

Rectifiability. Let λ_0 be a singular point for F_ε^λ at scale 1. We say that F_ε^λ is *rectifiable at* λ_0 if energies H_ε^p exist and a function $p = p(\lambda, \varepsilon)$ such that

(i) H_ε^p Γ-converge to H^p, and all p are regular points;

(ii) $F_\varepsilon^\lambda = H_\varepsilon^{p(\lambda,\varepsilon)}$ for (λ, ε) in a neighbourhood of $(0, \lambda_0)$.

The following theorem states that for rectifiable F_ε^λ a simple uniformly-equivalent family is given by H^p computed for $p = p(\lambda, \varepsilon)$.

Theorem. *Let F_ε^λ be rectifiable at λ_0; then F_ε^λ is uniformly equivalent to $G_\varepsilon^\lambda = H^{p(\lambda,\varepsilon)}$ at λ_0.*

Conclusions: construction of equivalent theories. From the analysis above we can sketch a procedure to construct equivalent families of parametrized functionals (*theories*) from a family F_ε^λ:

1. Identify *singular points* of F_ε^λ;
2. Compute the *table of* Γ*-limits* at singular points;
3. *Rectify* the energies at singular points;
4. *Match asymptotics*; i.e., construct energies that are uniformly equivalent to the Γ-limit (or Γ-development) far from singular points, and to the 'rectified' energies close to singular points.

Of course, the last point has not a unique answer, and additional criteria (simplicity, computability, closeness to well-known theories, etc) can drive it.

Remark The process above can be extended to the case when in place of the Γ-limit a development by Γ-convergence of F_ε^λ (see [1]) at some scale ε^α must be taken into account.

References

[1] G. Anzellotti and S. Baldo. Asymptotic development by Γ-convergence. *Appl. Math. Optim.* **27** (1993), 105-123.

[2] A. Braides. Γ-*convergence for Beginners*, Oxford University Press. Oxford, 2002.

[3] A. Braides. A handbook of Γ-convergence. In *Handbook of Differential Equations, Stationary Partial Differential Equations, Vol.* 3 (M. Chipot and P. Quittner eds.), Elsevier, 2006.

[4] A. Braides and L. Truskinovsky. Asymptotic expansions by Γ-convergence, *Cont. Mech. Therm.*, to appear.

[5] G. Dal Maso, *An Introduction to* Γ-*convergence*, Birkhäuser, Boston, 1993.

Super-hydrophobic strategies

David Quéré

Lotus or magnolia leaves and water striders legs have the common property of repelling water. In my talk, I discussed how microstructures at the surface of these materials induce this property. The nature of the design allows to generate related features, such as oil repellency rebound for impacting drops, or interfacial hydrodynamic slip. We concentrated on these unusual behaviors, and discussed which material design permits such special property. This is shown to be the first step for optimizing these surfaces - a question of current interest nowadays.

Creating materials with desired properties

A. G. Ramm

1. Introduction

Let $D \subset \mathbb{R}^3$ be a bounded domain, $n_0^2(x)$ be a continuous function in $\mathbb{R}^3$, $n_0^2(x) = 1$ in $D' := R^3 \backslash D$, $\operatorname{Im} n_0^2(x) \geq 0$. The scattering problem:

$$L_0 u_0 := [\nabla^2 + k^2 n_0^2(x)] u_0 = 0 \text{ in } \mathbb{R}^3, \qquad k = \text{const} > 0,$$
$$u_0(x) = e^{ik\alpha \cdot x} + v_0, \quad \frac{\partial v_0}{\partial r} - ikv_0 = o\left(\frac{1}{r}\right), \qquad r := |x| \to \infty,$$

has a unique solution. Here $\alpha \in S^2$ is the incident direction and v_0 is the scattered field. Define $q_0(x) := q_0(x,k) := k^2 - k^2 n_0^2(x)$. Since $k > 0$ is fixed, we drop the k-dependence of q_0. Then $L_0 = \nabla^2 + k^2 - q_0(x)$. The function $n_0^2(x)$ is called the refraction coefficient. We pose the following problem:

Problem 1. How does one create a material with a desired refraction coefficient $n^2(x)$ in D?

We prove that this is possible and give a recipe for doing this. If we know how to solve Problem 1, we can pose the following problems:

Problem 2. Can one create a new material in D with negative refraction?

Negative refraction means that the group velocity in D is directed opposite to the phase velocity.

Problem 3. Can one create a new material with a desired wave-focusing property?

This means that a plane wave at a fixed wavenumber $k > 0$ with a fixed incident direction α will have a desired far-field pattern.

Our theory contains answers to these questions.

2. Theory

2.1. We solve Problem 1 by embedding many particles (small bodies) $D_m = B(x_m, a) := \{x : |x_m - x| < a\}$, $D_m \subset D$, into D and requiring that in any open subset $\Delta \subset D$ the number of the embedded particles is given by the formula

$$\mathcal{N}(\Delta) = \frac{1}{a^{2-\kappa}} \int_\Delta N(x)\, dx \big[1 + \varepsilon(a)\big], \quad a \to 0, \tag{1}$$

where $0 < \kappa < 1$, $\lim_{a \to 0} \varepsilon(a) = 0$, and $N(x) \in C(D)$, $N(x) \geq 0$ is an arbitrary given function.

We assume that on the boundary S_m of D_m an impedance-type condition holds: $\frac{\partial u}{\partial N} = \frac{h(x_m)}{a^\kappa} u$, where $h(x) \in C(D)$, $\operatorname{Im} h(x) \leq 0$, is an arbitrary given function. Finally, we assume that the distance d between neighboring particles is of the order $O(a^{\frac{2-\kappa}{3}})$, $a \to 0$.

The scattering problem in the medium with M embedded particles is

$$
\begin{aligned}
&L_0 u_M = 0 \text{ in } \mathbb{R}^3 \backslash D, \qquad \frac{\partial u_M}{\partial N} = \frac{h(x_m)}{a^\kappa} u_M \text{ on } S_m, \quad 1 \le m \le M; \\
&u_M(x) = u_0(x) + v_M(x), \quad \frac{\partial v_M}{\partial r} - ikv_M = o\left(\frac{1}{r}\right), \qquad r \to \infty.
\end{aligned} \tag{2}
$$

Here N is the unit normal to S_m, $1 \le m \le M$, pointing out into D.

Define the effective field $u_e(x)$, $x \in D$:

$$
u_e(x) = \begin{cases} u_M(x) & \text{if } \lim\limits_{a \to 0} \dfrac{|x - x_m|}{a} = \infty, \ 1 \le m \le M, \\ u_M(x) - \int_{S_m} G(x,t)\sigma_m(t)\,dt & \text{if } \lim\limits_{a \to 0} \dfrac{|x - x_m|}{a} < \infty. \end{cases}
$$

Here $L_0 G = -\delta(x - y)$ in $\mathbb{R}^3$, G satisfies the radiation condition (2), and σ_m, $1 \le m \le M$, are the functions from the formula

$$
u_M(x) = u_0(x) + \sum_{m=1}^{M} \int_{S_m} G(x,t)\sigma_m(t)\,dt. \tag{3}
$$

Assume that (1) holds for the embedded particles $D_m \subset D$, and the boundary impedance of D_m is $\frac{h(x_m)}{a^\kappa}$, $0 < \kappa < 1$. Suppose that the functions $N(x) \ge 0$ in (1) and $h(x) = h_1 + ih_2$, $h_2 := \operatorname{Im} h \le 0$, are found from the equations

$$
h_1(x) = \frac{p_1(x)}{4\pi N(x)}, \quad h_2(x) = \frac{p_2(x)}{4\pi N(x)}, \tag{4}
$$

where $p(x) = p_1(x) + ip_2(x)$ is an arbitrary given function, $\operatorname{Im} p \le 0$. In (4) one may choose $N(x) > 0$ arbitrarily, and then $h_1(x)$ and $h_2(x)$ are uniquely defined by (4). Assume, finally, that the distance d between neighboring particles is $d = O(a^{\frac{2-\kappa}{3}})$, $a \to 0$.

Theorem. Under the above assumptions the new material in the domain D, created by the embedding of the small particles, has the refraction coefficient

$$
n^2(x) = n_0^2 - k^{-2} p(x). \tag{5}
$$

Since $p(x) = p_1 + ip_2$, $p_2 \le 0$, in the formula (4) is an arbitrary continuous function, the function $n^2(x)$ in (5) can be any desired function $n^2(x) \in C(D)$, $\operatorname{Im} n^2(x) \ge 0$.

2.2. By choosing $h = h(x, \omega)$ depending on ω, where $\omega > 0$ is the frequency, one can create $n^2(x, \omega)$ with a desired spatial dispersion, that is, with a desired dependence of $n^2(x, \omega)$ from ω. In particular, if $n(x, \omega) > 0$ and

$$
n + \omega \frac{\partial n}{\partial \omega} < 0, \tag{6}
$$

then the new material with the refraction coefficient $n^2(x, \omega) > 0$ has negative refraction, i.e., the group velocity $\nabla_k \omega$ is directed opposite to the phase velocity v_{ph}, where v_{ph} is directed along $k^0 = \nabla_k |k|$.

2.3. Given an arbitrary fixed $f(\beta) \in L^2(S^2)$, an arbitrary small fixed $\varepsilon > 0$, an arbitrary fixed $k_0 > 0$, and an arbitrary fixed $\alpha_0 \in S^2$, one can find $q \in L^2(D)$, $q = 0$ in $D' = R^3 \backslash D$, such that

$$\|A_q(\beta) - f(\beta)\|_{L^2(S^2)} < \varepsilon. \tag{7}$$

Here $A_q(\beta) := A_q(\beta, \alpha_0, k_0)$ is the scattering amplitude, corresponding to q, at fixed α_0 and k_0, and $q := k^2 - k^2 n^2(x)$. Given $f(\beta)$ and $\varepsilon > 0$, a method is given in [10] for finding $q(x)$ (nonuniquely!) so that (7) holds.

References

[1] A. G. Ramm, *Electromagnetic wave scattering by small bodies of arbitrary shapes*, in the book: "Acoustic, electromagnetic and elastic scattering-Focus on T-matrix approach" Pergamon Press, New York, 1980, pp. 537-546 (ed. V. Varadan).

[2] A. G. Ramm, *Wave scattering by small bodies of arbitrary shapes*, World Sci. Publishers, Singapore, 2005.

[3] A. G. Ramm, *Equations for the self-consistent field in random medium*, Phys.Lett. A, 312, N3-4, (2003), 256-261.

[4] A. G. Ramm, *Scattering by many small bodies and applications to condensed matter physics*, Europ. Phys. Lett., 80, (2007), 44001.

[5] A. G. Ramm, *Many-body wave scattering by small bodies and applications,* J. Math. Phys., 48, N10, (2007), 103511.

[6] A. G. Ramm, *Wave scattering by small impedance particles in a medium*, Phys. Lett. A 368, N1-2,(2007), 164-172.

[7] A. G. Ramm, *Distribution of particles which produces a "smart" material*, Jour. Stat. Phys., 127, N5, (2007), 915-934.

[8] A. G. Ramm, *Distribution of particles which produces a desired radiation pattern*, Physica B, 394, N2, (2007), 253-255.

[9] A. G. Ramm, *Creating wave-focusing materials, Inverse Problems, Design and Optimization,* Proceedings of the Intern. Symposium IPDO-2007, Vol. II, (2007), pp. 687-690. (Ed. G. Dulikravich et al).

[10] A. G. Ramm, *Inverse scattering problem with data at fixed energy and fixed incident direction*, Nonlinear Analysis: Theory, Methods and Applications, doi:10.1016/j.na.2007.06.047

[11] A. G. Ramm, *A recipe for making materials with negative refraction in acoustics*, Phys. Lett. A, doi:10.1016/j.physleta.2007.11.037

[12] A. G. Ramm, *Wave scattering by many small particles embedded in a medium*, Phys. Lett. A, (2008) doi: 10.1016/j.physleta.2008.01.006 (to appear)

Entropy of Microstructure

Victor Berdichevsky

This talk presents several points made in the author's papers [1] and [2].

•Thermodynamics concerns with the systems possessing at least two well separated time scales, and, thus, characterized by fast and slow variables. Thermodynamic theory is a theory of slow variables for such systems - this was one of major Boltzmann's insights. Ons can say that thermodynamic equations are the equations that are obtained by elimination of fast variables from the governing equations.

•Why the first and the second laws of thermodynamics hold true? The key reason is that the underlying governing equations are ergodic, mixing and Hamiltonian. Absence of ergodicity or Hamiltonian structure would prevent the existence on macrolevel temperature and entropy. Absence of mixing yields violation of the second law. These statements must be rectified in one respect: in fact, to have the laws of thermodynamics on macrolevel, the microequations might possesses slightly more general structure than the Hamiltonian one. It is not clear though, if that has any physical significance, because the Hamiltonian structure of microequations is supported by all existing experimental evidences.

•We call the laws of thermodynamics obtained by elimination of fast degrees of freedom from Hamiltonian equations primary thermodynamics. The characteristic features of primary thermodynamics are the appearance of two new slow variables, temperature and entropy, and the dissipation of energy of slow variables (the total energy of fast and slow variables is conserved in isolated systems). It is essential, that, under some assumptions, the equations for slow variables possess a Hamiltonian structure, if dissipation is negligible. That indicates the existence of quite peculiar "Hamiltonian reciprocities" in macrophysical interactions. This feature is a constraint for macroequations which is additional to the first two laws of thermodynamics and to Onsager's reciprocity principle, which is called sometimes the third law of thermodynamics.

• The dissipative equations of primary thermodynamics can also possess two well separated time scales. Two examples are plasticity and turbulence. In plasticity of metals, the equations of primary thermodynamics are the equations of dislocation dynamics (dislocation motion is usually slow compared with the motion of atoms of crystal lattices). In turbulence, the averaged characteristics of fluid flow change slowly on the characteristic time scale of velocity fluctuations. Elimination of fast degrees of freedom in primary thermodynamics yield the equations of secondary thermodynamics.

•If the fast variables in primary thermodynamics perform some chaotic motion, then, after elimination of fast degrees of freedom and transition to the secondary thermodynamics, two new slow variables appear, "secondary entropy" and "secondary temperature". Their physical contents depend on the particular area. In what follows, we consider micromechanics of solids, and the corresponding parameters are called microstructure entropy and microstructure temperature.

•By materials with microstructure we understand further the inhomogeneous materials with the characteristic size of inhomogeneity much smaller than the characteristic length of the macro-problem. To model the behavior of such materials, one uses some finite set of parameters describing geometrical and physical features of microstructure, denote these parameters by $\rho_1, ..., \rho_k$. The problem that arises in modeling of micro-inhomogeneous materials is that energy is not determined uniquely by any finite set of the parameters. We have to admit that energy, E, can take different values for different samples even if these samples have the same values of parameters, $\rho_1, ..., \rho_k$. Thus, energy becomes a random number and has some probability density function, $f(E \mid \rho_1, ..., \rho_k)$. We define entropy of

microstructure, $\mathcal{S}_m(E, \rho_1, ..., \rho_k)$, by the Einstein-type formula,

$$f(E \mid \rho_1, ..., \rho_k) = const\, e^{\mathcal{S}_m(E, \rho_1, ..., \rho_k)}. \tag{1}$$

Entropy of microstructure characterizes scattering of energy for a set of parameters used to describe the microstructure.

•There are two qualitatively different situations in modeling of micro-inhomogeneous bodies: entropy of microstructure, $\mathcal{S}_m(E, \rho_1, ..., \rho_k)$, can be a smooth function of E or it may have a sharp maximum. In the latter case $\mathcal{S}_m$ contains a large factor, N,

$$\mathcal{S}_m(E, \rho_1, ..., \rho_k) = NS_m(E, \rho_1, ..., \rho_k), \tag{2}$$

while $S_m(E, \rho_1, ..., \rho_k)$ is a smooth function of E. As some examples show, the large parameter, N, has the meaning of a "number of inhomogenuities" in the random structure: $N = |V| / a^3$, a being the correlation radius of the microstructure.

In the case (2), the most probable value of energy, $\hat{E}$, appears with overwhelming probability. At this value function $\mathcal{S}_m(E, \rho_1, ..., \rho_k)$ has maximum over E for fixed $\rho_1, ..., \rho_k$. The most probable value of energy, $\hat{E}$, is a function of $\rho_1, ..., \rho_k$,

$$\hat{E} = \hat{E}(\rho_1, ..., \rho_k). \tag{3}$$

Equation (3) can be considered as the equation of state of the body. Since energy, up to small fluctuations, is a function of $\rho_1, ..., \rho_k$, the parameters, $\rho_1, ..., \rho_k$, may be viewed as the thermodynamic parameters of the system.

The case when entropy of microstructure, $\mathcal{S}_m(E, \rho_1, ..., \rho_k)$, does not have sharp maximum is different: energy becomes an independent parameter of state additional to the parameters, $\rho_1, ..., \rho_k$. To return to the usual framework of classical thermodynamics, we have to admit that there is an additional parameter of state which "absorbs" the arbitrariness of energy for given $\rho_1, ..., \rho_k$, entropy of microstructure, $\mathcal{S}_m$, and

$$E = E(\mathcal{S}_m, \rho_1, ..., \rho_k). \tag{4}$$

Function (4) can be viewed as the inversion of the function $\mathcal{S}_m(E, \rho_1, ..., \rho_k)$ introduced by (1).

•To find entropy of microstructure experimentally, one has to consider many samples, to measure for each sample the values of the parameters, $E, \rho_1, ..., \rho_k$, determine probability density function and compute entropy of microstructure from (1). In the case of crystal plasticity, when one is interested in modeling of motion and nucleation of crystal defects, energy can be found experimentally, as was suggested by Taylor and Quinney, by comparing the amount of heat needed to melt the sample and the corresponding defectless monocrystal.

•In two examples (elastic bar, consisting of many sections with random properties, and small random Gaussian disturbance of homogeneous media) microstructure entropy was computed analytically.

• The concept of microstructure entropy seems quite important for modeling of macrobehavior of micro-inhomogeneous bodies. An attempt to apply this concept in modeling of plasticity of metals was made in [2]. For metals, the microstructure

is the dislocation network, which evolves in the course of deformation. Modeling was based on the assumption that microstructure entropy in an isolated system has the tendency to decrease. Perhaps, this feature is of quite general nature, and microstructure entropy of any isolated system decreases in time (in most cases, i.e. if the initial conditions are not specially prepared).

References

[1] Berdichevsky, V.: Structure of equations of macrophysics. Phys. Rev. E **68**, 066126, (2003).
[2] Berdichevsky, V.: Entropy of microstructure. J. Mech. Phys. Solids, doi:10.1016/j.jmps.2007.07.004 (2007).

Electronic Structure Calculations at Macroscopic Scales

Michael Ortiz

(joint work with K. Bhattacharya, T. Blesgen, V. Gavini, J. Knap, P. Suryanarayana)

Density functional theory (DFT) has provided insights into a broad range of material properties. However its computational complexity has made bulk properties, especially those involving defects, beyond reach. We have developed a computational scheme that enables the study of multi-million atom clusters using orbital-free DFT (OFDFT) with no spurious physics or restrictions on geometry. The key ideas are: (i) a real space formulation of DFT; (ii) a nested finite element implementation of the formulation, and (iii) a systematic means of adaptive coarse-graining, retaining full resolution where necessary and coarsening elsewhere with no patches, assumptions or structure. We have demonstrated the method, its accuracy under modest computational cost and the physical insights it offers by means of several applications involving clusters, vacancies, di-vacancies and prismatic dislocation loops in aluminium

Relaxation and microstructure formation in single-crystal plasticity

Sergio Conti

This talk discussed several applications of relaxation theory to models from the deformation theory of crystal plasticity. The deformation theory of plasticity is appropriate for loadings which lead to a locally monotone evolution of the internal variables, and confers the boundary value problem of plasticity a well-defined variational structure analogous to elasticity. The discreteness of the slip directions in crystals introduces a nonconvex constraint, leading to the formation of fine-scale structures.

We first study a geometrically nonlinear problem with a single slip system, both without and with linear hardening. Then the plastic strain takes the form $\mathrm{Id} + \gamma s \otimes m$, where s and m are a fixed pair of orthonormal vectors in $\mathbb{R}^2$ and $\gamma \in \mathbb{R}$. For simplicity we consider an elastically rigid problem, i.e. assume that the elastic part of the deformation is a rotation, and neglect dissipation. For both

cases, the quasiconvexification of the energy density can be determined in closed form.

Theorem 1 (joint work with Florian Theil, see [5]). *The quasiconvex envelope of the function*

$$W_s(F) = \begin{cases} |\gamma| & \text{if } F = Q(\mathrm{Id} + \gamma s \otimes m) \quad Q \in SO(2) \\ \infty & \text{else.} \end{cases} \tag{1}$$

is given by

$$W_s^{qc}(F) = \begin{cases} \lambda_2(F) - \lambda_1(F) & \text{if } \det F = 1 \text{ and } |Fs| \leq 1 \\ \infty & \text{else.} \end{cases}$$

Here $\lambda_1(F)$ and $\lambda_2(F)$ denote the singular values of F, i.e., the ordered eigenvalues of U in the polar decomposition $F = QU$, $Q \in SO(2)$, $U = U^T$.

We remark that the function $F \mapsto \lambda_2(F) - \lambda_1(F)$ is isotropic, even if the problem is clearly anisotropic. The orientation of the slip system survives in the relaxation only through the condition $|Fs| \leq 1$. This is different in the case with self hardening.

Theorem 2 (From [2]). *The quasiconvex envelope of the function*

$$W_r(F) = \begin{cases} \gamma^2 & \text{if } F = Q(\mathrm{Id} + \gamma s \otimes m) \quad Q \in SO(2) \\ \infty & \text{else.} \end{cases} \tag{2}$$

is given by

$$W_r^{qc}(F) = \begin{cases} |Fm|^2 - 1 & \text{if } \det F = 1 \text{ and } |Fs| \leq 1 \\ \infty & \text{else.} \end{cases}$$

In the case of two slip systems the situation becomes substantially more complex. The rank-one convex envelope can still be determined in closed form.

Theorem 3 (joint work with Nathan Albin and Georg Dolzmann, see [1]). *The rank-one convex envelope W^{rc} of*

$$W(F) = \begin{cases} |\gamma| & \text{if } F = Q(\mathrm{Id} + \gamma e_1 \otimes e_2) \text{ for some } \gamma \in \mathbb{R}\,, \;\; Q \in SO(2)\,, \\ |\gamma| & \text{if } F = Q(\mathrm{Id} + \gamma e_2 \otimes e_1) \text{ for some } \gamma \in \mathbb{R}\,, \;\; Q \in SO(2)\,, \\ \infty & \text{otherwise} \end{cases}$$

is given by

$$W^{\mathrm{rc}}(F) = \begin{cases} (\lambda_2 - \lambda_1)(F) & \text{if } \det F = 1, \min\{|Fe_1|, |Fe_2|\} \leq 1, \\ \psi(|Fe_1|, |Fe_2|) & \text{if } \det F = 1, 1 \leq |Fe_1| \leq |Fe_2|, \\ \psi(|Fe_2|, |Fe_1|) & \text{if } \det F = 1, 1 \leq |Fe_2| \leq |Fe_1|, \\ \infty & \text{if } \det F \neq 1, \end{cases}$$

where

$$\psi(\alpha, \beta) = \int_1^\alpha \frac{2s^2}{\sqrt{s^4 - 1}}\, ds + \frac{1}{\alpha}\left(\sqrt{\alpha^2\beta^2 - 1} - \sqrt{\alpha^4 - 1}\right).$$

The relaxation is obtained with infinite-order laminates, partially supported at infinity. This means that slip concentration is expected, with microstructure on infinitely many length scales. Numerical estimates have shown that second-order laminates are sufficient to achieve $W^{\rm rc}$ within 2%, see [1] for details.

We then discuss a problem with many slip systems, within a linearized framework. Precisely, let $S = \{s_i \otimes m_i\}_{i=1,\dots N}$ be a set of slip systems, each (s_i, m_i) being an orthonormal pair in $\mathbb{R}^3$; the set S is assumed to be sufficiently large (see [4] for details; the usual sets for fcc and bcc metals satisfy this assumption). Let $u : \Omega \subset \mathbb{R}^3 \to \mathbb{R}^3$ be the deformation, $\gamma : \Omega \to \mathbb{R}^N$ be the set of internal variables. We assume no self-hardening and positive latent-hardening. Precisely, let

$$\Gamma_s = \left\{\gamma \in \mathbb{R}^N : \exists j, \gamma_i = 0 \ \ \forall i \neq j\right\}$$

be the set of single-slip slip parameters. Then we consider a latent hardening function $f_{LH} : \mathbb{R}^N \to [0, \infty]$ such that $f(\gamma) = 0$ for $\gamma \in \Gamma_s$. We focus on the condensed energy

$$W_{\rm cond}(\epsilon) = \min_{\gamma \in \mathbb{R}^N} \left\{ \frac{1}{2}(C(\epsilon - \epsilon_p(\gamma)), \epsilon - \epsilon_p(\gamma) + \tau \sum_{i=1}^{N} |\gamma_i| + f_{LH}(\gamma) \right\},$$

where the plastic strain takes the form

$$\epsilon_p(\gamma) = \sum_{i=1}^{N} \gamma_i \frac{s_i \otimes m_i + m_i \otimes s_i}{2}.$$

The variational problem amounts at minimizing

$$E[u] = \int_\Omega W_{\rm cond}\left(\frac{\nabla u^T + \nabla u}{2}\right) dx$$

subject to appropriate boundary conditions. We show that the quasiconvex envelope of $W_{\rm cond}$ equals its convex envelope. This determines also the relaxation of $E[u]$.

Theorem 4 (joint work with M. Ortiz, see [4])**.** *The quasiconvex envelope of the function $W_{\rm cond}$ equals its convex envelope*

$$W^{**}_{\rm cond}(\epsilon) = \min_{\gamma \in \mathbb{R}^N} \left\{ \frac{1}{2}(C(\epsilon - \epsilon_p(\gamma)), \epsilon - \epsilon_p(\gamma) + \tau \sum_{i=1}^{N} |\gamma_i| \right\}$$

(both functions of strain are understood to be composed with projection onto symmetric matrices).

We remark that $W^{**}_{\rm cond}(\epsilon)$ corresponds to the case of zero latent hardening, i.e., to $W_{\rm cond}$ for $f_{LH} = 0$. This means that, by developing microstructures in the form of sequential laminates of finite depth, crystals can *beat* the single-slip constraint, i. e., the relaxed constitutive behavior is indistinguishable from multislip ideal plasticity. In turn, this means that, within this model, latent hardening has no effect on the macroscopic material properties. An application of this relaxation

result to finite-element simulations of an indentation test has been discussed in [3]

References

[1] Albin, N., Conti, S., and Dolzmann, G. Infinite-order laminates in a model in crystal plasticity. preprint.
[2] Conti, S. Relaxation of single-slip single-crystal plasticity with linear hardening. In *Multiscale Materials Modeling* (Freiburg, 2006), P. Gumbsch, Ed., Fraunhofer IRB, pp. 30–35.
[3] Conti, S., Hauret, P., and Ortiz, M. Concurrent multiscale computing of deformation microstructure by relaxation and local enrichment with application to single-crystal plasticity. *Multiscale Modeling and Simulation 6* (2007), 135–157.
[4] Conti, S., and Ortiz, M. Dislocation microstructures and the effective behavior of single crystals. *Arch. Rat. Mech. Anal. 176* (2005), 103–147.
[5] Conti, S., and Theil, F. Single-slip elastoplastic microstructures. *Arch. Rat. Mech. Anal. 178* (2005), 125–148.

Fluctuations in micro (and macro) scale plasticity

Michael Zaiser

Plasticity of crystalline solids proceeds in a sequence of intermittent bursts with power-low size distribution. We give examples for this behavior and then discuss a variety of computational models capable of reproducing the phenomenon. Common ingredients of these models are (i) the existence of long-range interactions with a tendency of "smoothing" the deformation field, (ii) spatially random flow thresholds that are either inherited from randomized initial conditions or put in "by hand" in form of given quenched disorder, and (iii) external driving that is either done with a stiff/mixed device or fine tuned to a critical driving force. Under these circumstances, all models discussed show burst sequences with power-law statistics, their exponents bring those of the critical branching process.

An introduction to the Sandpile model

Frank Redig

We introduce the BTW model and discuss its basic mathematical structure such as abelian group, burning algorithm, spanning trees. We also discuss the connection with so called activated walker problem as proposed by Dickman and others.

A plasticity theory of solids in the presence of phase transitions

Thomas Blesgen
(joint work with Isaac V. Chenchiah)

This work deals with binary phase transitions and the formation of microstructure in solids that undergo plastic deformations, possibly accompanied by diffusion, for a constant temperature θ.

One application of the developed theory is the class of metallic-intermetallic laminates, see [5], [6]. The model is formulated within the framework of rate-independent finite-strain elasto-plasticity, going back to [1], [4]. In contrast to existing work, like e.g., [2], the stored mechanical energy $\overline{W}$ is also considered a function of an external phase parameter $\chi \in BV(\Omega; \{0,1\})$. Here, $\Omega \subset \mathbb{R}^3$ denotes the reference domain which is assumed to be a bounded set with Lipschitz boundary.

The deformations are represented by a mapping

$$\varphi : \Omega \times [0,T] \to \Omega_t,$$

with $\Omega_t := \{\varphi(x,t) \,|\, x \in \Omega\}$ the deformed domain at time t.

The transformation $F := D\varphi$ is decomposed as $F = F_{\mathrm{e}}F_{\mathrm{p}}$ into an elastic part F_{e} and a plastic part F_{p} with F_{e}, $F_{\mathrm{p}} \in GL(\mathbb{R}^3)$ and we set $P := F_{\mathrm{p}}^{-1}$. Additionally, a latent hardening variable $\kappa \in L^2(\Omega; \mathbb{R})$ is introduced.

The stored mechanical energy is supposed to depend only on the elastic part of F and be frame indifferent. One example is the class of Neo-Hookean materials

$$\overline{W}(\chi, \kappa, F_{\mathrm{e}}) = \frac{\nu(\chi)}{2}\|F_{\mathrm{e}}\|^2 + \frac{\eta}{2}\kappa^2 + U(\det F_{\mathrm{e}}),$$

where $\nu(\chi) > 0$ is the Lamé parameter, $\eta > 0$ the hardening coefficient, and U is a convex functional with $U(d) \to \infty$ for $d \to 0$ and $d \to \infty$.

Next we introduce the set of dual variables

$$\xi = -\frac{\partial W}{\partial \chi}, \quad \pi = -\frac{\partial W}{\partial \kappa}, \quad T = \frac{\partial W}{\partial F}, \quad X = -\frac{\partial W}{\partial P}$$

and introduce a yield function $Y = Y_{x,D\chi}(\xi, \pi, \overline{X}) \leq 0$. The condition $Y = 0$ is a prerequisite for plasticity. The von Mises condition reads for instance

$$Y_{x,D\chi}(\xi, \pi, \overline{X}) := \|\mathrm{dev}\ \mathrm{sym}\overline{X}\| - \sigma_Y - \pi + |\xi|\mathcal{X}_{S(D\chi)}.$$

Here, $S(D\chi)$ is a measurable, material-dependent set that designates the possible regions of plasticity in Ω.

The principle of maximal plastic dissipation leads to the flow rule

$$(\partial_t\chi, \partial_t\kappa, P^{-1}\partial_t P) \in \partial^{\mathrm{sub}} Q_{x,D\chi}(\xi, \pi, \overline{X}) \tag{1}$$

where ∂_{sub} denotes the subdifferential and the plastic potential is

$$Q_{x,D\chi}(\xi, \pi, \overline{X}) := \begin{cases} 0 & \text{for } Y_{x,D\chi}(\xi, \pi, \overline{X}) \leq 0, \\ \infty & \text{else.} \end{cases}$$

Notice that according to (1), the phase variable χ changes rapidly due to mechanical forces.

We introduce densities $\varrho_i : \Omega \times [0,T] \to \mathbb{R}^+$ that determine the density of the i-th species, whereas ϱ_0 determines the density of vacancies. Let ψ_k denote the specific free energy of phase k which is a convex function of ϱ and let

$$\mu := \sum_k \chi_k \frac{\partial \psi_k}{\partial \varrho}(\varrho)$$

be the chemical potential. For fixed $h > 0$ we pass to a time-discrete formulation, [3], where for instance $\partial_t^h \chi := (\chi(t) - \chi(t-h))h^{-1}$. If ψ_k^*, Q^* denote the Legendre-Fenchel transforms of ψ_k, Q, we find the total free energy of the system to be

$$\Psi(\mu,\chi,\kappa,\varphi,P)(t) := \int_\Omega |D\chi| + \overline{W}(\chi,\kappa,D\varphi P) + \psi^\star(\mu,\chi) + hQ^\star_{x,D\chi(t-h)}(\partial_t^h\chi, \partial_t^h\kappa, d_t^h(P))\,\mathrm{d}x.$$

We minimize Ψ in suitable spaces subject to the constraint

$$\partial_t \varrho_i(x,t) + \varrho_i(x,t)\mathrm{div}(\partial_t\varphi(x,t)) = \mathrm{div}(L\nabla\mu(x,t))_i \qquad \text{in } \Omega \tag{2}$$

rewritten as a condition on μ.

To study the properties of the model, we consider the example of one active slip system. Let m, $n \in \mathbb{R}^3$ be given unit vectors with $m \cdot n = 0$ such that $P = \mathrm{Id} + \gamma m \otimes n$. Let $C := F^t F$ and $C_{mm} := m \cdot Cm$, $C_{mn} := m \cdot Cn$. We find that the free energy minimization becomes for the first time step

$$\Psi(\mu,\chi,\kappa,\varphi,\gamma)(t) = \int_\Omega \psi^\star(\mu,\chi) + |D\chi| + U(\sqrt{\det C}) + \frac{\nu(\chi)}{2}\left(\mathrm{tr}C + 2C_{mn}\gamma + C_{mm}\gamma^2\right) + \frac{\eta}{2}\kappa^2 + \sigma_Y|\gamma - \gamma_0|\,\mathrm{d}x \to \min$$

subject to the constraints: (2) on μ and

$$\begin{aligned} |\gamma - \gamma_0| + \kappa - \kappa_0 &\le 0, \\ |\chi - \chi_0| \le |\gamma - \gamma_0| &\qquad \text{in } S(D\chi_0), \\ \chi = \chi_0 &\qquad \text{in } \Omega \setminus S(D\chi_0). \end{aligned}$$

More specifically, we consider the case of a shear of 45 degrees w.r.t. the chosen slip system and let $F(x) = \mathrm{Id} + \frac{\alpha(x)}{2}(n+m)\otimes(n-m)$. The dependence of α on $x \in \Omega$ allows for microstructure.

We explicitly compute the minimizer. Let

$$K(\chi) := \{x \in S(D\chi_0) \,|\, |\chi(x) - \chi_0(x)| = 1\}$$

be the subset of Ω where the constraint on χ is active.

It can be shown that in $\Omega \setminus K$, the integrand of Ψ is non-convex in α for η small enough and convex in α for η large. Thus hardening opposes to the generation of micro-structure.

In $K(\chi)$ we find that the integrand of Ψ is convex in α. Consequently, no microstructure exists in the set $K(\chi)$, i.e. in the set that has been passed in the last time step by the transition layer.

The behavior sketched in the above examples can also be observed in other cases like the von Mises condition. Finally, the effect of diffusion can be studied numerically for these examples and it can be made explicit how the minimizers depend on the choice of L.

References

[1] R. Hill, *A general theory of uniqueness and stability in elastic-plastic solids*, Journal Mech. Phys. Solids, **6** (1958), 236–249

[2] R.D. James, *Finite Deformation by mechanical twinning*, Arch. Rational Mech. Anal., **77** (1981), 143–176

[3] M. Ortiz, L. Stainier, *The variational formulation of viscoplastic constitutive updates*, Comp. Methods Appl. Mech. Engrg., **171** (1999), 419–444

[4] J.R. Rice, *Inelastic constitutive relations for solids: an internal-variable theory and its applications to metal plasticity*, Journ. Mech. Phys. Solids, **19** (1971), 433–455

[5] K.S. Vecchio, R.R. Adharapurapu, F.C. Jiang, *Effects of ductile laminate thickness, volume fraction, and orientation of fatigue-crack propagation in Ti-Al3Ti metal-intermetallic laminate*, Metallurgical and Materials Transactions A, **36** (2005), 1595–1608

[6] T. Li, F. Jiang, E.A. Olevsky, K.S. Vecchio, M.A. Meyers, *Damage evolution in Ti6Al4V-Al_3Ti metal-intermetallic laminate composites*, Materials Science and Engineering A, **443** (2007), 1–15

Dynamics and nucleation of dislocations in crystals

Ana Carpio

(joint work with Luis L. Bonilla, Ignacio Plans)

Periodized discrete elasticity models [1, 2, 3] are the simplest correction to linear elasticity equations allowing for nucleation and motion of dislocations in crystals. Two ingredients are needed to build a periodized discrete elasticity model for a particular type of crystal. First a linear lattice model reproducing the crystal structure and yielding the correct linear anisotropic elasticity equations in the continuum limit has to be found. To this end, an adequate potential energy for the crystal lattice is defined. This may be done by thinking of the crystal as a set of balls joined by springs or by discretizing the continuous elastic energy using the crystal lattice as a mesh. Next, the periodicity of the crystal has to be restored, allowing atoms to change neighbors. This could be done by a nonlinear relabelling protocol. From an analytical point of view, it is more convenient to introduce periodic functions of discrete differences along the primitive directions of the crystal with a period equal to the lattice constant.

These models are useful to understand nucleation and motion of dislocations (defects supported by lines) in nanocrystals at low temperatures. In heteroepitaxial growth, for instance, layers of atoms of a new crystal are grown on a substrate. After a few layers, a barrier of misfit dislocations is formed. In a different context, nanoindentation tests use the tip of an electronic microscope to apply a load on the surface of a nanocrystal. Past a critical stress, dislocations are generated around the tip. These crystals are perfect except for a few dislocations moving along primitive directions of the crystal. Secondary slip systems are only activated at large temperatures and high strain rates. Nanoindentation tests provide information on the nanocrystal mechanical properties and on incipient plasticity.

Compared to standard molecular dynamics models, the mathematical structure of periodized discrete elasticity models allows for cheaper simulations and an elementary analysis. By construction, the perfect crystal is a stable equilibrium. Pinned edge and screw dislocations are stationary solutions behaving at infinity like singular solutions of the Navier equations [1, 4]. Moving dislocations are travelling wave solutions [5]. Dislocations interact as expected. For example, if we have a set of planar edge dislocations with parallel Burgers vectors along the x axis, dislocations having the same sign of the Burgers vector repel each other. Dislocations whose Burgers vectors have opposite signs attract and they either cancel each other or form dipoles and loops. In simple geometries, a more precise analysis can be done.

Let us consider a 2D cubic lattice for which only displacements in the x direction are relevant. The lattice evolution is governed by the nondimensional equations:

$$\begin{aligned} m\frac{d^2u_{i,j}}{dt^2}+\alpha\frac{du_{i,j}}{dt} &= u_{i+1,j}-2u_{i,j}+u_{i-1,j} \\ &+ \frac{A}{2\pi}\left[\sin(2\pi(u_{i,j+1}-u_{i,j}))+\sin(2\pi(u_{i,j-1}-u_{i,j}))\right], \end{aligned} \tag{1}$$

where $u_{i,j}$ represents the dimensionless displacement of the atom (i,j) in the direction x. Periodicity is only needed in the direction in which changes of neighbors can take place. We have selected a sine function. In practice, this periodic function would have to be fitted to the material. The lattice spacing is normalized to 1. Here $A = C_{44}/C_{11}$ for a cubic crystal with elastic constants C_{11}, C_{12}, C_{44}.

This simple model allows for nucleation and motion of edge dislocations along the x direction when a shear stress of strength F is applied in the x direction. Dislocation depinning can be characterized as a global bifurcation [6], explaining the role of stationary and dynamic Peierls stresses [5, 7, 8]. Dislocation nucleation appears as a subcritical pitchfork bifurcation, yielding the critical stress for nucleation, the nucleation site and the nature of nucleated defects [9].

Dislocation depinning. Let us consider a lattice containing an edge dislocation. We apply a shear stress of strength F in the x direction. Stationary dislocation solutions are constructed by looking for stationary solutions that behave at infinity like $\theta(i, \frac{j}{\sqrt{A}}) + Fj$, θ being the angle function. For small F, the resulting solutions take values in the region where the sine function is increasing. Existence of stationary dislocations can be proven using a maximum principle for the overdamped

version of (1) and constructing adequate sub and supersolutions [4]. Above a threshold, the spatial operator changes type and dislocations start to move.

Two critical values of the stress are found. Below F_s, stable stationary dislocation solutions exist. Above F_d, stable travelling dislocations are found. In general, $F_d < F_s$. Both thresholds only agree in the overdamped limit $m = 0$. In this case, a prediction of the dislocation speed is found by assembling the information available above and below threshold. The linear stability analysis of the stationary dislocation solutions shows that the largest negative eigenvalue vanishes at F_s. The corresponding bifurcation is a global saddle-node bifurcation, and the solution can be approximated by matched asymptotic expansions in the limit as $F \to F_s+$ (for $F > F_s$ the dislocation moves as a traveling wave). The amplitude equation corresponding to a saddle-node bifurcation has solutions that blow up in finite time as $F \to F_s-$. At the blow-up times, the solution described by the amplitude equation has to be matched to an inner solution that solves (1) with $F = F_s$ and appropriate matching conditions. The profiles of the travelling dislocations are step-like; see [1, 6] for details. A numerical calculation of the traveling wave shows that as F approaches F_s from above, its profile develops steps, which become steeper and steeper near F_s where the previously described approximation based on the global bifurcation applies. The speed of the wave is related to the time one atom spends in a step, which can be estimated using the normal form of the bifurcation. This yields a $(F - F_s)^{1/2}$ scaling for the speed. The scaling changes to 3/2 in the presence of spatial disorder. It would also be affected by temporal fluctuations, if present; see [5] and references therein. When $m \neq 0$, predicting a speed law requires the analysis of a bifurcation in the branch of travelling waves.

Homogeneous nucleation. Let us now analyze homogeneous nucleation of dislocations by shearing a dislocation-free state. When $F = 0$, $u_{i,j} = 0$ is a stable solution corresponding to a perfect crystal. As F is increased, we find a branch BR0 of stationary solutions representing sheared lattices without defects. Numerical continuation indicates that this branch becomes unstable at a critical shear stress F_n. At this point, a subcritical pitchfork bifurcation takes place. Two new branches of stationary configurations, BR1 and BR2, appear. Both are initially unstable, but become stable for stresses larger than F_n^1 and F_n^2, respectively. BR1 represents nucleation of one dipole, which splits in two edge dislocations moving towards the boundary of the lattice. BR2 corresponds to nucleation of two dipoles, that split in four edge dislocations. Since F_n^1 and F_n^2 are smaller than F_n, nucleation can occur before reaching F_n. The final pattern observed in dynamical tests depends on the way the load is applied. If we deform a lattice at a large strain rate, one dipole is nucleated. At low strain rates, two dipoles are observed. The eigenfunction corresponding to the zero eigenvalue of the linear stability problem at F_n locates the nucleation site. Nucleation starts in the region where the eigenfunction takes large values. The two different patterns correspond to perturbations of the lattice configuration at F_n by either adding or subtracting multiples of the eigenfunction. Dipoles split because the critical stress for nucleation is much larger than the critical stress for edge dislocation depinning.

In an isotropic crystal, our critical stress for nucleation scales as $\frac{\mu}{4}$, comparable to Taylor's estimate for the theoretical strength of a crystal. The factor $\frac{1}{4}$ depends on our choice of periodic interaction. Though homogeneous nucleation has long be thought to be an elastic instability at finite strength, no precise analysis of this instability had been carried out up to now. Preliminary tests in more complex indentation or fracture settings suggest that a similar analysis is possible.

References

[1] L.L. Bonilla, A. Carpio, *Defects, singularities and waves*, Recent Advances in Nonlinear Partial Differential Equations and Applications, Serie "Proceedings of Symposia in Applied Mathematics", **65**, AMS (2007), 131-150.

[2] L.L. Bonilla, A. Carpio, I. Plans *Dislocations in cubic crystals described by discrete models*, Physica A **376** (2007), 361-377.

[3] A. Carpio, L.L. Bonilla *Discrete models for dislocations and their motion in cubic crystals*, Phys. Rev. B **71** (2005), 134105, 1-10.

[4] A. Carpio *Wavefront solutions for discrete two dimensional nonlinear diffusion equations*, Appl. Math. Lett. **15** (2002), 415-421.

[5] A. Carpio, L.L. Bonilla *Edge dislocations in crystal structures considered as traveling waves of discrete models*, Phys. Rev. Lett. **90** (2003), 135502, 1-4.

[6] A. Carpio, L.L. Bonilla *Depinning transitions in spatially discrete reaction-diffusion equations*, SIAM J. Appl. Math **63** (2003), 1056-1082.

[7] A. Carpio *Nonlinear stability of oscillatory wave fronts in chains of coupled oscillators*, Phys. Rev. E **69** (2004), 046601, 1-13.

[8] A. Carpio, L.L. Bonilla *Oscillatory wave fronts in chains of coupled nonlinear oscillators*, Phys. Rev. E **67** (2003), 056621, 1-11.

[9] I. Plans, A. Carpio, L.L. Bonilla, *Homogeneous nucleation of dislocations in a periodized discrete elasticity model*, Europhysics Letters **81** (2008), 36001, 1-6.

Variational Models for Plasticity by Homogenization of Discrete Dislocations

Adriana Garroni

(Joint work with G. Leoni and M. Ponsiglione)

The presence of crystal defects like dislocations (and their motion) is consider the main mechanism of plastic deformations in metals. In the linearized theory the elastic energy of a body Ω in presence of plastic deformations is obtained by decomposing the displacement gradient, $\nabla u = \beta^e + \beta^p$, in the elastic and the plastic strain respectively, and computing

$$\int_\Omega W(\nabla u - \beta^p)\, dx\,,$$

where $W(\xi)$ is the anisotropic linear elastic energy density. Various phenomenological models have been proposed to account for the plastic effects due to dislocations, as the so called strain gradient theories (see e.g. [3] and [4]). In view of the topological nature of the dislocations, their presence can be modeled in the continuum by assigning the Curl of the field β^p. The quantity $\mathrm{Curl}\beta^p = \mu$ is then called the dislocation density. Inspired by this idea, the strain gradient

theory for plasticity, assigns an energy to the plastic deformation depending on the dislocation density, so that the energy looks like

$$\int_\Omega W(\nabla u - \beta^p)\,dx + \int_\Omega \varphi(\mathrm{Curl}\beta^p)\,dx\,. \tag{1}$$

The purpose of the term depending on $\mathrm{Curl}\beta^p$ is to introduce an internal scale penalizing oscillations of the dislocation density. The main issue is the choice of the function φ. In fact the usual choice ([3],[4]) is to take φ quadratic. This choice of the function φ makes the energy (1) regular but has the well known disadvantage of preventing concentration of the dislocation density. In view of this observation other models propose a positively 1-homogeneous behavior, as the L^1 norm of $\mathrm{Curl}\beta^p$ (see e.g. [5] and [2]), that is less tractable in some respects, but has the feature of allowing patterns formations of dislocation walls.

Our aim is to derive model (1) starting from a model of discrete dislocations which accounts for the crystalline structure and considering only the elastic distortion induced by a given distribution of dislocations. We consider a 2-dimensional domain Ω (the cross section of a cylindrical 3-dimensional domain) in which straight dislocations are identified with points $x_i \in \Omega$ or, more precisely, with a small region surrounding the dislocation referred to as the *core region*, i.e., a ball $B_\varepsilon(x_i)$, being the core radius ε proportional to the underlying lattice spacing. The presence of the dislocations can be detected looking at the topological singularities of a continuum strain field β, i.e.,

$$\int_{\partial B_\varepsilon(x_i)} \beta \cdot t\,ds = b_i\,, \tag{2}$$

where t is the tangent to $\partial B_\varepsilon(x_i)$ and b_i belongs to a set S of admissible Burgers vectors (for square crystals, up to renormalization, $S = \{\mathbf{e}_1, \mathbf{e}_2, -\mathbf{e}_1, -\mathbf{e}_2\}$). To any such a strain field β we associate the following elastic energy

$$\int_{\Omega_\varepsilon} W(\beta)\,dx\,, \tag{3}$$

where $\Omega_\varepsilon = \Omega \setminus \cup_i B_\varepsilon(x_i)$.

It is well known that the self energy of a single dislocation is of the order $|\log\varepsilon|$, while the interaction energy between two dislocations is much smaller. When the number of dislocations increases the interaction energy becomes more relevant and in the regime where the number of dislocations is of order $|\log\varepsilon|$ the two terms (the self and the interaction energy) balance. We then scale the energy (3) by $|\log\varepsilon|^2$ and study the Γ-limit as $\varepsilon \to 0$, considering the distribution of dislocations as a variable of the problem.

In our analysis we introduce a second small scale $\rho_\varepsilon \gg \varepsilon$ (the *hard core radius*) at which a cluster of dislocations will be identified with a multiple dislocation. In mathematical terms this corresponds to introduce the span $\mathbb{S}$ of S on $\mathbb{Z}$ (i.e., the set of finite combinations of Burgers vectors with integer coefficients) and represent a

generic distribution of dislocations as a measure μ of the type

$$\mu = \sum_{i=1}^{N} \delta_{x_i} b_i, \qquad b_i \in \mathbb{S}\,,$$

where the distance between the x_i's is at least $2\rho_\varepsilon$. The admissible strain fields β corresponding to μ are defined outside the core region, namely in $\Omega_\varepsilon(\mu) = \Omega \setminus \cup_i B_\varepsilon(x_i)$, satisfy (2), and the corresponding energy functional is given by

$$F_\varepsilon(\mu, \beta) = \frac{1}{|\log \varepsilon|^2} \int_{\Omega_\varepsilon(\mu)} W(\beta)\, dx\,. \tag{4}$$

Under a suitable condition on the hard core scale we can show that in the asymptotics this energy can be decomposed into two effects: the *self energy*, concentrated in the hard core region (i.e. $\cup_i B_{\rho_\varepsilon}(x_i)$) and the *interaction energy*, diffused in the remaining part of Ω. The Γ-limit of F_ε is then given by

$$\int_\Omega W(\beta)\, dx + \int_\Omega \varphi\left(\frac{d\mu}{d|\mu|}\right) d|\mu|\,, \tag{5}$$

where the function φ is positively homogeneous of degree 1 and it is defined by a suitable asymptotic cell problem formula. The first term is the elastic energy of the limiting rescaled strain and represents the interaction energy. The second term represents the self energy and depends only on the rescaled dislocation density $\mu = \mathrm{Curl}\beta$. This constraint implies that the measure μ must belong to the space $H^{-1}(\Omega; \mathbb{R}^2)$. In particular concentration on lines is permitted accounting for the presence of pattern formations as *dislocation walls*. An additional feature of this limit is the anisotropy of the self energy density inherited from the anisotropic elastic tensor and the class of the admissible Burgers vectors accounting for the crystalline structure.

References

[1] Cermelli P., Leoni G., Energy and forces on dislocations. SIAM J. Math. Anal. 37 (2005), no. 4, 1131-1160.

[2] S. Conti and M. Ortiz, Dislocation Microstructures and the Effective Behavior of Single Crystals, Archive Rat. Mech. Anal., 176 (2005), 103-147.

[3] Fleck N. A. and Hutchinson J. W., A phenomenological theory for strain gradient effects in plasticity, Journal of the Mechanics and Physics of Solids 41 (1993), 1825-1857

[4] Gurtin M. E., On the plasticity of single crystals: free energy, microforces, plastic-strain gradients, Journal of the Mechanics and Physics of Solids 48 (2000), 989-1036.

[5] Ortiz M. and Repetto E. A., Nonconvex energy minimization and dislocation structures in ductile single crystals, J. Mech. Phys. Solids 47 (1999), 397-462.

[6] Ponsiglione M., Elastic energy stored in a crystal induced by screw dislocations: from discrete to continuum, SIAM J. Math. Anal. 39 (2007), no. 2, 449-469.

[7] E. Sandier and S. Serfaty, Limiting Vorticities for the Ginzburg-Landau Equations, Duke Math J., 117, No 3, (2003), 403-446.

Active gels: Statistical Physics of active systems

Jean-François Joanny
(joint work with Frank Jülicher, Karsten Kruse, Jacques Prost)

Active systems are systems which are maintained in a non-equilibrium state by injection of energy. The energy is then either used to produce work or is consumed as heat. Active systems exist at various scales. At a macroscopic scale assemblies of animals such as bird flocks or fish colonies show spectacular collective behaviors where all individuals are moving in a coordinated motion. Similarly, bacterial colonies are active systems which dissipate energy by consuming oxygen. Vibrated granular materials can also be considered as active systems with an energy input due to the mechanical vibration; they show various instabilities and spontaneous organization. At a more microscopic level, biological systems such as cells consume the energy of chemical reactions such as the hydrolysis of AdenosineTriPhosphate (ATP) into AdenosinDiPhosphate and inorganic phosphate. This energy is used for example by motor proteins to generate forces and produce motion.

Our work focuses on the cytoskeleton which is the gel-like structure that provides the elasticity of cells. The main components of the cytoskeleton are actin filaments and myosin II molecular motors. From a polymer point of view the actin filaments form a physical gel with an elastic modulus of the order of 10^4Pa. The gel is polar because the individual actin filaments are polar The molecular motors create internal stresses inside the gel and tend to contract it.

We have constructed a generalized hydrodynamic theory of polar active gels [1, 3, 2] in order to describe the mechanical properties of the cytosekleton. Hydrodynamic theories consider the behavior of a system at large length scales and over long time scales. They ignore the microscopic details and are only based on symmetries. The dynamic behavior of the system is characterized by a set of phenomenological dissipative coefficients such as viscosities or mobilities. Although the examples of active systems that we have given have very different characteristic length scales and time scales they all share the same polar symmetry and one can hope to describe them by the same hydrodynamic theory. Of course the transport coefficients will have very different values. The determination of the transport coefficients from the properties of the individual component of the system requires a microscopic theory which is specific to each active system.

The hydrodynamic theory is constructed by following the lines introduced for the hydrodynamics of liquid crystals by Martin and coworkers [4]. By considering the free energy dissipation, we identify fluxes and forces and we write the most general linear relationship between fluxes and forces that respects the symmetries (including the time reversal symmetry). The choice of what are considered as fluxes or forces is somehow arbitrary. Considering the stress as a flux, the conjugated force is the velocity gradient. We describe the visco-elasticity of the cytoskeleton by the simple Maxwell model which involves a single relaxation time. The polarity of the actin gel is characterized by a polarization vector field p_α. The associated flux is the rate of change of the polarization and the conjugated force is

the orientational field acting on the polarization. Finally, we want to describe the activity. The associated flux is the number of ATP molecules consumed per unit time and unit volume and the conjugated force is the energy gained per hydrolyzed ATP molecule $\Delta\mu$. We consider here that cells regulate the concentrations of ATP and ADP molecules and that $\Delta\mu$ has a fixed value. This seems to be a reasonable approximation.

The general Onsager relation between fluxes and forces involves several transport coefficients but all coefficients are not independent in a linear theory due to the Onsager symmetry relations. Most of these coefficients however have their equivalents for nematic liquid crystals or elastomers and experimental techniques have been proposed to measure them. The only new transport coefficients are the active coefficients giving the dependence on the activity $\Delta\mu$. If the cytoskeleton is considered as incompressible, there are only two active coefficients corresponding to an active stress and and active orientational field. The active stress can be written as $\sigma_{\alpha\beta} = -\zeta\Delta\mu p_\alpha p_\beta$ it describes the internal stresses created by the myosin motors pulling on the crosslinks of the actin gel. Comparison with experiments on motility of lamellipodia, gives an order of magnitude of 10^3Pa for the active gel i.e. ten times smaller than the elastic modulus. The active orientational field is associated to the action of molecular motors pulling two filaments to drive them parallel.

Activity has spectacular effects on the hydrodynamics of active polar gels. The active stress depends on the local polarization. Any gradient of polarization therefore creates a stress gradient which in turn induces flow. A gradient of polarization can be created by imposing different orientations of the two surfaces of a thin film. If the film is active even in the absence of any pressure gradient, the film flows due to the induced polarization gradient. Even if the polarization on the two surfaces of a film is parallel to the surfaces, the film can flow if its thickness is large enough. The homogeneous state where the polarization is everywhere parallel to the surface and the film does not flow is only stable for small film thickness. If the thickness of the film is large enough, the homogeneous steady state is unstable, the polarization spontaneously tilts and the films flows. This instability studied in Ref.[5] is very similar to the Frederics transition if liquid crystals.

The basic theory of active gels presented here has been generalized to gels comprising several constituents or to take into account thermal and non-thermal fluctuations. We are currently using this theory to study properties of cells such as cell motility or the instabilities associated to cortical actin.

References

[1] K. Kruse, J.F. Joanny, F. Jülicher, J. Prost, and K. Sekimoto, *Eur. Phys. J. E* **16**, 5 (2005).
[2] F. Jülicher, K. Kruse, J. Prost and J.F. Joanny *Physics Reports* **449**, 3 (2007).
[3] J.F. Joanny, F. Jülicher, K. Kruse and J. Prost *New Journal of Physics* **9**, 422 (2007).
[4] P.C. Martin, O. Parodi, and P. Pershan,*Phys. Rev. A* **6**, 2401 (1972).
[5] R. Voituriez, J.F. Joanny, and J. Prost, *Eur. Phys. Lett.* **70**, 404 (2005).

Diffusions in one dimensional space and time periodic drifts

Pierre Collet
(joint work with Servet Martínez)

We have considered four models for the diffusion of a particle in a periodic drift. The first model is a simple diffusion with density distribution $u(t,x)$ evolving according to

$$\partial_t u(t,x) = D\partial_x^2 u(t,x) + \partial_x\big(b(t,x)u(t,x)\big) \ ,$$

where the drift b is space and time periodic with average zero in both variables. The constant $D>0$ is the diffusion coefficient. This equation was proposed as a simple model for molecular motors and appears also in other situations (see [2] for a review and references).

This density evolution corresponds to the stochastic differential equation

$$dX = -b(t,X)dt + \sigma dW(t) \ ,$$

where W is the Brownian motion.

We are mostly interested in the existence and properties of an average asymptotic velocity defined by

$$I(b) = \lim_{t\to\infty} \frac{1}{t}\int x\, u(t,x)dx \ , \tag{1}$$

provided the limit exists.

A second model considers a particle evolving in a landscape which is still periodic in space but can be this landscape can be in two states. The landscape flips from one state to the other as a continuous time Markov process (see [2] for a review and references). In each state the landscape drift (the functions b_1 and b_2 below) is assumed to be periodic in space and of average zero but independent of time. Two functions $\rho_1(t,x)$ and $\rho_2(t,x)$ represent the density distribution of the particle when the landscape is in state 1 and 2 respectively. The evolution equations are given by

$$\begin{aligned} \partial_t\rho_1 = &\ \partial_x\big(D\partial_x\rho_1 + b_1(x)\rho_1\big) - \nu_1\rho_1 + \nu_2\rho_2 \\ \partial_t\rho_2 = &\ \partial_x\big(D\partial_x\rho_2 + b_2(x)\rho_2\big) + \nu_1\rho_1 - \nu_2\rho_2 \ . \end{aligned}$$

The constant $D>0$ is the diffusion coefficient, and the constants $\nu_1>0$ and $\nu_2>0$ are the transition rates of the landscape. In this case one is interested in the average asymptotic velocity defined by

$$I\big(b_1,b_2\big) = \lim_{t\to\infty}\frac{1}{t}\int x\,\big(\rho_1(t,x)+\rho_1(t,x)\big)dx \ ,$$

The two other models are the analogs of the previous ones when inertia is taken into account (Kramers equation instead of Fokker-Planck-Kolmogorov equations).

Our third model for example is given by the Langevin equation

$$\begin{aligned} dx = &\ v\,dt \\ dv = &\ \big(-\gamma\, v + F(t,x)/m\big)\,dt + \sigma\, dW_t \end{aligned}$$

where x and v are the position and velocity of the particle, $\gamma > 0$ a friction coefficient, m the mass of the particle and $F(t,x)$ the exterior force assumed to be periodic and with average zero in both variables. The number $\sigma > 0$ is the standard deviation of the noise, and W_t the Brownian motion.

In all cases we define an average asymptotic velocity I analogous to (1), and we consider this quantity as a function of the drift(s).

For the case of C^1 drift(s), we have established analogous theorems for the four models. The first result is that the functional $I(b)$ is well defined (the limit in the definition always exist and is independent of the initial condition satisfying some natural assumption). Moreover, this functional is real analytic in the drift and non trivial (the non triviality is established by looking at the Taylor expansion at the origin). The proof is based on a reduction to a problem on the circle (some kind of homogenisation), also reminiscent of the theory of Floquet multipliers. Here the dominant multiplier is one because of conservation of probability. Analyticity is established using analytic perturbation theory.

A direct consequence is that the functional $I(b)$ does not vanish on a dense open set. Although there is no explicit formula for the value of $I(b)$ at a given b (not even for the sign), the result implies a local stability of this velocity. We refer to [1] for details.

References

[1] P.Collet, S.Martinez. Asymptotic velocity of one dimensional diffusions with periodic drift. To appear in Journal of Mathematical Biology, `arXiv:0705.1435`.

[2] P.Reimann. Brownian motors: noisy transport far from equilibrium. Physics Report **361**, 57-265 (2002).

A primer in inhomogeneity and growth

Marcelo Epstein

The purpose of this presentation was to provide a unified treatment of certain theories of material inhomogeneities, on the one hand, and of evolution and growth, on the other hand. The common background is supplied by their placement within the general framework of continuum mechanics and by the use of differential geometric tools. The formulation of the theory of material inhomogeneity is based on the one proposed by Noll [2] and Wang [3] as far back as 1967. When understood in the context of the differential geometry of G-structures and groupoids, the theory is amenable to rather straightforward generalizations in several directions, including structured media of various kinds and general relativity. Central to the theory is the concept of material isomorphism, a concept that expresses the precise meaning of the notion of equal material response of two points, regardless of the reference state used to describe that response. The interplay between material isomorphism and material symmetry is then revealed and shown to play a crucial role in the theory. Within the larger framework of groupoids, both material isomorphisms and material symmetries can be regarded as similar notions, much

in the same way that a tiled floor may have local symmetries (at the level of each tile) and distant symmetries (when comparing two separate tiles). A body all of whose points are mutually materially isomorphic is said to be materially uniform. A convenient way to express mathematically the idea of material uniformity is by specifying a field of implants from an externally placed material archetype to each of the body points. A uniform body is homogeneous if it can be brought to a configuration in which the material response of all points is identical. In other words, the material implants constitute a constant field relative to the Euclidean structure of the surrounding space. Analytically, this idea corresponds to an integrability condition which has also a clear geometric counterpart in terms of the vanishing of some characteristic geometric object. The time-like counterpart of the theory of material uniformity is that of material evolution of the so-called anelastic type, such as it occurs in the classical theory of plasticity and in certain theories of volumetric growth. It is shown that, within this context, the Eshelby tensor emerges naturally as the configurational force thermodynamically associated with the evolution of a first-grade material. In a similar way, the J-integral of fracture mechanics appears in the expression of the translation of an inhomogeneity with compact support. When proposing evolution laws as first-order differential equations for the implant maps, it can be shown that these laws must be subject to certain formal restrictions, such as the law of actual evolution that specifies that a true evolution must yield a time-derivative of the implant maps that does not belong to the Lie algebra of the symmetry group of the archetype. The somewhat controversial issue of the possible need for extra balance laws for the configurational forces driving the evolution is analyzed under the umbrella of the second law of thermodynamics and it is suggested that the formulation of such laws is, at least in some cases, equivalent to the introduction of ad-hoc entropy sinks as part of the specification of the parameters of an essentially open system. A detailed treatment can be found in [1].

References

[1] Epstein M, Elzanowski M (2007) Material inhomogeneities and their evolution, Springer-Verlag

[2] Noll W (1967) Materially uniform bodies with inhomogeneities, *Archive for Rational Mechanics and Analysis* 27: 1–32

[3] Wang C-C (1967) On the geometric structure of simple bodies, a mathematical foundation for the theory of continuous distributions of dislocations, *Archive for Rational Mechanics and Analysis* 27: 33–94

Sticky foliations and shock waves

Yann Brenier

The non self penetrating condition (NSPC in short) in Continuum Mechanics is hard to handle because it is usually not a convex constraint. However, when the "material" is made of a foliation of leaves of codimension one (i.e. hypersurfaces),

each of them being supposed to be non self penetrating, the only condition to satisfy is that these leaves must stay well ordered in the one-dimensional transversal dimension.

Let us consider the simplest case, when the leaves are just graphs $y = Y(t, x, a) \in R$, where a denotes the label of each leave (say $a \in [0, 1]$ for simplicity), $x \in R^d$ and the surrounding space is just $(x, y) \in R \times R^d$. Then, the NSPC just reads $\partial_a Y \geq 0$ and we can call "sticky zone" the set $(t, x, y = Y(t, x, a))$ where $\partial_a Y(t, x, a) = 0$. This convex constraint can be encoded by the convex potential $\Phi_0[Y]$ with value 0 as $\partial_a Y \geq 0$ and $+\infty$ otherwise. Notice that this potential can be approximated by a smoother one such as

$$\Phi_\epsilon[Y] = \epsilon \int \varphi(\partial_a Y(x, a))dxda,$$

as $\epsilon \to 0$, where $\varphi(\tau)$ is any convex function on the real line, with values $+\infty$ if $\tau < 0$, smooth for $\tau > 0$. Typical examples are:

$$\varphi(\tau) = \tau \log \tau, \quad \varphi(\tau) = -\log \tau + \tau, \quad \varphi(\tau) = 1/\tau + \tau.$$

Now, the idea is to consider evolution laws for each leave that are not necessarily compatible, in the large, with the NSPC. The simplest situation is when each leave, of label a, moves at constant speed, say $V(a) \in R^d$ along the x axis and $W(a) \in R$ along the y axis, which leads (ignoring the NSPC) to

$$Y(t, x, a) = Y(t = 0, x - tV(a), a) + tW(a),$$

or, in PDE words,

$$(1) \qquad \partial_t Y + V(a) \cdot \nabla_x Y = W(a).$$

Taking into account the NSPC can be done just by including the constraint potential into (1), namely

$$(1s) \qquad W(a) \in \partial_t Y + V(a) \cdot \nabla_x Y + \partial\Phi_0[Y],$$

borrowing notations from Convex Analysis. This subdifferential equation is easy to handle, mathematically speaking, and is well posed in L^2. The same is true for the approximate equation obtained by substituting Φ_ϵ for Φ_0:

$$(1\epsilon) \qquad \partial_t Y + V(a) \cdot \nabla_x Y = W(a) + \epsilon \partial_a(\varphi'(\partial_a Y)).$$

Then we can prove the following Theorem [1]:

Let Y be a solution to (1s). Then

$$u(t, x, y) = \int_0^1 1\{Y(t, x, a) \leq y\}da$$

is an entropy solution, in the sense of Kruzhkov [2], of the hyperbolic nonlinear conservation law:

$$(2) \qquad \partial_t u + \nabla \cdot (F(u)) + \partial_y(G(u)) = 0,$$

where

$$F(a) = \int_0^a V(b)db, \quad G(a) = \int_0^a W(b)db,$$

and the sticky zone of Y corresponds to the shock set of u.

The class of equations (2) includes the famous inviscid Burgers equation as $F = 0$ (or $d = 0$) and $G(u) = u^2/2$. There is an interesting additional feature when we approximate Φ_0 by Φ_ϵ. Let us consider the simplest case when $d = 0$ (no x variable). Then, we can, at least formally, rewrite equation (1ϵ) as:

$$\partial_{tt} Y = \epsilon \partial_a (\varphi''(\partial_a Y)\partial_a \partial_t Y).$$

Introducing the corresponding Eulerian velocity and density fields

$$v(t, Y(t,a)) = \partial_t Y(t,a), \quad \rho(t, Y(t,a)) = 1/\partial_a Y(t,a),$$

we get the Eulerian version of (1ϵ):

$$\partial_t \rho + \partial_y(\rho v) = 0,$$

$$\rho(\partial_t v + v\partial_y v) = \epsilon \partial_y(\mu(\rho)\partial_y v),$$

where $\mu(\rho) = 1/\rho\varphi''(1/\rho)$ can be interpreted as a viscosity coefficient and comes up for very natural mathematical reasons.

References

[1] Y. Brenier, *L2 formulation of multidimensional scalar conservation laws*, http://arxiv.org/pdf/math.AP/0609761.

[2] M. Muster, *Computing other invariants of topological spaces of dimension three*, S.N. Kružkov, *Generalized solutions of the Cauchy problem in the large for first order nonlinear equations*, Soviet Math. Dokl. 10 (1969), 785–788.

Three observations on stationary heat conduction in moderately rarefied gases

Ingo Müller

i. Fourier theory compared to 13-moment theory

Grad's thirteen moment distribution function is a reliable tool for the determination of the temperature field in a moderately rarefied gases, when steep temperature gradients occur. The distribution function reads

$$f_G = f_{equ}(1 + \underbrace{\frac{1}{\rho\frac{k}{\mu}T} t_{\langle ij\rangle}(\frac{1}{\frac{k}{\mu}T} C_i C_j - \delta_{ij}) - \frac{1}{\rho(\frac{k}{\mu}T)^2} q_i C_i (1 - \frac{1}{5}\frac{1}{\frac{k}{\mu}T} C^2)}_{\varphi})$$

where $t_{\langle ij\rangle}$ is the deviatoric stress and q_i the heat flux. The 13-moment field equations can be solved explicitly in the case of heat conduction between concentric cylinders for either Maxwellian molecules, or for the BGK-ansatz. For the latter the temperature field reads

$$T = c_2 - \frac{c_1}{5\frac{k}{\mu}\tau p} \ln(\frac{28}{25}\frac{\tau}{p} c_1 + r^2)$$

For specific boundary values for the heat flux at the inner cylinder and the temperature at the outer one, Fig. 1a shows the temperature field according to this theory. It deviates from the one of the classical Fourier theory of heat conduction, where the temperature gradient is steep.

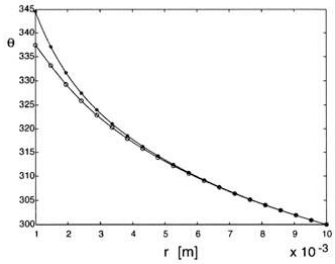

FIGURE 1. Temperature fields of thirteen moment theory and Fourier theory

ii. Kinetic and thermodynamic temperatures

Temperature is supposed to be a measure for the mean kinetic energy of the atoms of a body. On the other hand, in thermodynamics, temperature is defined as the quantity that is continuous at a heat conducting wall. The latter definition is called the zeroth law of thermodynamic. That definition is often equivalent to the continuity of the entropy flux at a heat conducting wall. This is indeed the case, if the entropy flux is given by $\frac{q_i}{T}$.

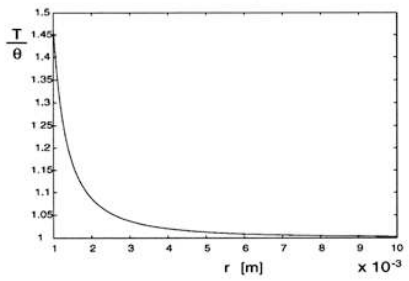

FIGURE 2. Comparison of kinetic and thermodynamic temperatures.

However, in the thirteen moment theory the entropy flux turns out to be given by

$$\Phi_i = \frac{q_i}{T} + \frac{2}{5}\frac{t_{\langle ij\rangle}q_j}{pT}$$

or, for the problem of heat conduction between concentric cylinders by

$$\Phi(1) = \underbrace{\frac{1}{T}(1 + \frac{2}{5}\frac{t_{\langle 11\rangle}}{p})q_1}_{\frac{1}{\Theta}}$$

Therefore, if the entropy flux is continuous, so is the quantity Θ, identified by the brace in the equation. Obviously in equilibrium, where $t_{\langle 11\rangle}$ vanishes, T and Θ are equal. But that is not the case outside equilibrium. Θ is the measurable quantity by virtue of its continuity, and - if measured – it should differ appreciably from T as Fig 2 shows.

iii. Heat conduction in a rotating frame.

The Boltzmann equation contains inertial terms due to the centrifugal force, the Coriolis force, etc. acting on the atoms in a non-inertial frame during their free path. That frame dependence is reflected in the 13-moment equations, and it produces quantitative and qualitative differences from the classical Navier-Stokes-Fourier theory. Thus for heat conduction between concentric cylinders the inertial terms make it impossible for a gas to participate in a rigid rotation of the cylinders. In other words: A gas cannot rotate rigidly, if it conducts heat. There is an azimuthal velocity field between the cylinders.

The 13-moment theory permits the calculation of the azimuthal velocity field and Fig 3 shows its graphs for different values of the pressure, i.e. for different degrees of rarefaction.

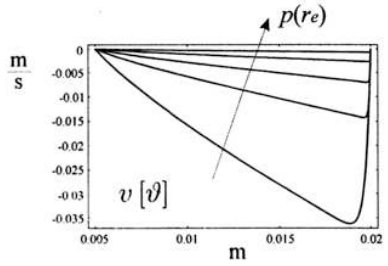

FIGURE 3. Azimuthal velocity field between concentric cylinders in a non-inertial frame.

REFERENCES

[1] Müller, I. Ruggeri, T. *Stationary heat conduction in radially symmetric situations - an application of extended thermodynamics.* Journal of Non-Newtonian Fluid Mechanics **119** (2004)

[2] Barbera, E. Müller, I. *Secondary heat flow between confocal ellipses - an application of extended thermodynamics.* Journal of Non-Newtonian Fluid Mechanics (in press)

[3] Barbera, E. Müller, I. *Inherent frame dependence of thermodynamic fields in a gas.* Acta Mechanica, **184** (2006)

Boundary conditions and Knudsen layers for moment equations of rarefied gas dynamics

Henning Struchtrup

The equations of classical hydrodynamics, the Navier-Stokes-Fourier equations, cannot describe rarefaction effects in gases, which appear in processes with Knudsen numbers $\mathrm{Kn} > 0.1$. A variety of extended models which aim at describing rarefied gas flows at least approximately was derived from the Boltzmann equation. The best known among these are the Burnett and super-Burnett equations, derived by means of the Chapman-Enskog method, and Grad's 13 moment equations, which follow from Grad's moment method. However, Burnett and super-Burnett equations suffer from instabilities in transient processes. Grad's moment equations exhibit unphysical sub-shocks in shock structures at large Mach numbers [1].

Techniques for the regularization of Grad's 13 moment equations leads to the so-called regularized 13 moment equations (R13), which are stable and guarantee smooth shock structures [2][3]. The derivation of the R13 equations by means of the *order of magnitude method* [4][5] allows to relate the equations to powers in the Knudsen number. The method was developed up to the third order for the special case of Maxwell molecules, and yields the Euler equations at zeroth order, the Navier-Stokes-Fourier equations at second order, Grad's 13 moment equations (with omission of a non-linear term) at second order, and the regularization of these (R13) at third order. The Burnett and super-Burnett equations can be recovered from the R13 equations by means of a Chapman-Enskog expansion.

The order of magnitude method was also employed to study slow non-isothermal flows [6].

Boundary conditions were the major obstacle in simulations based on advanced continuum models of rarefied and micro-flows for a long time. A theory to combine the regularized 13-moment-equations with boundary conditions based on Maxwell's accommodation model was only presented recently [7]. The boundary conditions are derived from the hypothesis that the equations have to be adapted to the boundary conditions in a way that the number of boundary conditions required does not depend on the process. This consistency requirement is necessary, since the number of boundary conditions differs between the fully non-linear and the linearized 13 moment equations.

The complete set of boundary conditions for the linear equations follows from taking suitable moments of the boundary condition for the Boltzmann equation. Additional boundary conditions for the non-linear equations are derived from the equations in the bulk, by transforming them while keeping their asymptotic accuracy with respect to the Boltzmann equation.

Comparison between numerical solutions for the R13 equations with the new boundary conditions with Discrete Simulation Monte Carlo solutions of the Boltzmann equation show very good agreement.

The existence of an H-theorem was proven at least for the linearized R13 equations, both for the bulk and the boundary conditions [8].

A particular feature of models for rarefied flows is the occurrence of Knudsen boundary layers in the solutions. A detailed study of the Knudsen layers in a simplified kinetic model for phonon energy transfer [9] shows that the Knudsen layer contributions do not obey the scaling of the Chapman-Enskog expansion and the order of magnitude method, which therefore cannot be used to reduce the number of moments in Knudsen layers. However, the study shows that Knudsen layers can be reasonably well described by few moments as long as the Knudsen number of the problem does not exceed unity.

Acknowledgment: This research was supported by the Natural Sciences and Engineering Research Council (NSERC).

References

[1] H. Struchtrup, *Macroscopic Transport Equations for Rarefied Gas Flows—Approximation Methods in Kinetic Theory.* Interaction of Mechanics and Mathematics Series, Springer, Heidelberg 2005

[2] H. Struchtrup and M. Torrilhon, Regularization of Grad's 13-moment-equations: Derivation and Linear Analysis, *Phys. Fluids* **15**, 2668–2680 (2003)

[3] M. Torrilhon and H. Struchtrup, Regularized 13-Moment-Equations: Shock Structure Calculations and Comparison to Burnett Models, *J. Fluid Mech.* **513**, 171–198 (2004)

[4] H. Struchtrup, Stable transport equations for rarefied gases at high orders in the Knudsen number, *Phys. Fluids* **16** (2004), 3921–3934

[5] H. Struchtrup, Derivation of 13 moment equations for rarefied gas flow to second order accuracy for arbitrary interaction potentials, *Multiscale Model. Simul.* **3**, 211-243 (2004)

[6] H. Struchtrup, Scaling and expansion of moment equations in kinetic theory, *J. Stat. Phys.* **125**(3), 565-587 (2006)

[7] M. Torrilhon and H. Struchtrup, Boundary Conditions for Regularized 13-Moment-Equations for Micro-Channel-Flows, *J. Comp. Phys., published online* 17 October 2007, doi:10.1016/j.jcp.2007.10.006

[8] H. Struchtrup and M. Torrilhon, H-theorem, regularization, and boundary conditions for linearized 13 moment equations, *Phys. Rev. Lett.* **99**, 014502 (2007)

[9] H. Struchtrup, Linear Kinetic Heat Transfer: Moment Equations, Boundary Conditions, and Knudsen layers, *Physica A*, doi:10.1016/j.physa.2007.11.044 (2007)

Invariance equation for model reduction in dissipative systems

Alexander N. Gorban

(joint work with Iliya V. Karlin, Andrei Y. Zinovyev)

In this talk I would like to review the theory of *invariance equation* and application of this theory to model reduction in dissipative systems. Invariance equation is a condition of invariance of an immersed manifold f_M with respect to a given vector field $J(f)$ (Fig. 1).

Perhaps, the first important result about this equation was the Lyapunov auxiliary theorem about analytical invariant manifolds near an equilibrium (a zero of $J(f)$) [1]. Recently, this theorem is intensively used for model reduction [2]. The Chapman–Enskog method for the Botzmann equation [3] is just a formal solution of the invariance equation using the asymptotic expansion in the powers of a small parameter (the Knudsen number). Later, Fenichel [4] transformed the

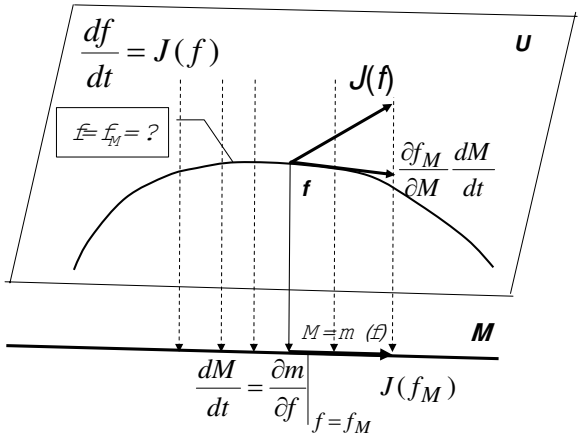

FIGURE 1. Invariance equation: f is vector of microscopic variables (detailed description), $M = m(f)$ is vector of macroscopic variables (reduced description), $M \mapsto f_M$ is immersion ($m(f_M) = M$), condition of invariance is $J(f_M) = \frac{\partial f_M}{\partial M}\frac{dM}{dt}$ or in more detail

$$J(f_M) = \frac{\partial f_M}{\partial M}\frac{\partial m(f)}{\partial f}\bigg|_{f=f_M} J(f_M)$$

Chapman–Enskog method into "geometric singular perturbation" theory, but for finite-dimensional vector fields. The famous Kolmogorov–Arnold–Moser theory could be considered as the theory of invariance equations for almost integrable Hamiltonian systems. Kolmogorov proposed to use fast Newton type methods for solving this equation instead of power series [5]. We applied this idea to dissipative systems (the Boltzmann equation), and this allowed us to resolve some of classical problems which appears in the Chapman–Enskog expansion (negative viscosity and short waves instability in higher approximations, etc.) [6].

Almost 20 years ago several groups of researchers started to develop constructive methods for model reduction using invariant manifolds [7, 8, 9, 10, 11]. Some of these technics are specially compared on benchmarks [12, 13]. There exist now 5 groups of methods for computation of *slow invariant manifold*.

(1) Power series expansion (a) in powers of a small parameter (the Chapman–Enskog expansion for the Boltzmann equation and the Fenichel theory of geometric singular perturbations) or (b) in powers of phase variables (Lyapunov series);
(2) The Newton-type methods;
(3) Relaxation methods (the Euler method for the immersed manifolds auxiliary motion, for example);

(4) Method of natural projector (extension of the Hilbert method for the Boltzmann equation);
(5) Discretization of the invariance equation and invariant grids.

The method of natural projector was introduces as a generalization of the Ehrenfests' coarse-graining [14]. Independently, similar idea was developed into so-called "Equation-free, coarse-grained multiscale computation" [15]. The equation of the auxiliary motion of the immersed manifold f_M is

$$\frac{df_M}{d\tau} = J(f_M) - \frac{\partial f_M}{\partial M}\frac{\partial m(f)}{\partial f}\bigg|_{f=f_M} J(f_M).$$

The right-hand side of this equation is the residual of the invariance equation (*defect of invariance*). Steady states of this equation are invariant manifolds, and stable steady states are supposed to be slow invariant manifolds. This definition (*slowness as stability*) is the reason why the relaxation methods can be applied for slow invariant manifolds construction.

There exist reviews and books [16, 17, 18, 19] about invariance equation and numerous applications. (Here we touched applications to dissipative systems only.) Nevertheless, this equation remains "the great unknown equation". Why? Perhaps, because it has huge amount of solutions and the rules for selection of the proper solution are not obvious. Lyapunov used analyticity. Indeed, near a non-resonant fixed point this is a good rule (as is follows from the Lyapunov auxiliary theorem). We can use also stability in various senses, and can try to build new criteria of slowness. Summation and resummation of power series can also help [20]. But the theory of the invariance equation (for model reduction) is far from being complete: we only begin now to understand the proper questions.

References

[1] A.M. Lyapunov, The general problem of the stability of motion, Taylor & Francis, London, 1992.
[2] Kazantzis, N., Kravaris, C., Nonlinear observer design using Lyapunov's auxiliary theorem, Systems Control Lett., **34** (1998), 241–247.
[3] Chapman, S. and Cowling, T., Mathematical theory of non-uniform gases, Third edition, Cambridge University Press, Cambridge, 1970.
[4] Fenichel, N., Persistence and smooothness of invariant manifolds for flows, Indiana Univ. Math. J., **21** (1971), 193–226.
[5] A.N. Kolmogorov, On conservation of conditionally periodic motions under small perturbations of the Hamiltonian. Dokl. Akad. Nauk SSSR, **98** (1954), 527–530.
[6] A.N. Gorban and I.V. Karlin, Method of invariant manifolds and regularization of acoustic spectra, Transport Theory and Stat. Phys., **23** (1994), 559–632.
[7] C. Foias, M.S. Jolly, I.G. Kevrekidis, G.R. Sell, and E.S. Titi, On the computation of inertial manifolds, Physics Letters A, **131**, 7–8 (1988), 433–436.
[8] M.R. Roussel and S.J. Fraser, Geometry of the steady–state approximation: Perturbation and accelerated convergence methods, J. Chem. Phys., **93** (1990), 1072–1081.
[9] A.N. Gorban and I.V. Karlin, Thermodynamic parameterization, Physica A, **190** (1992), 393–404.
[10] U. Maas and S.B. Pope, Simplifying chemical kinetics: intrinsic low– dimensional manifolds in composition space, Combustion and Flame, **88** (1992), 239–264.

[11] S.H. Lam and D.A. Goussis, The CSP Method for Simplifying Kinetics, International Journal of Chemical Kinetics, **26** (1994), 461–486.
[12] A. Zagaris, H.G. Kaper, and T.J. Kaper, Analysis of the computational singular perturbation reduction method for chemical kinetics, Journal of Nonlinear Science, **14**, 1 (2004), 59–91.
[13] E. Chiavazzo, A.N. Gorban, and I.V. Karlin, Comparison of invariant manifolds for model reduction in chemical kinetics, Commun. Comput. Phys. 2 (5) (2007), 964–992
[14] Gorban, A.N., Karlin, I.V., Öttinger, H.C., and Tatarinova, L.L., Ehrenfest's argument extended to a formalism of nonequilibrium thermodynamics, Phys.Rev.E **63** (2001), 066124.
[15] I.G. Kevrekidis, C.W. Gear, J.M. Hyman, P.G. Kevrekidis, O. Runborg, and C. Theodoropoulos, Equation-free, coarse-grained multiscale computation: enabling microscopic simulators to perform system-level analysis, Comm. Math. Sci., **1** 4 (2003), 715–762.
[16] A.N. Gorban and I.V. Karlin, Method of invariant manifold for chemical kinetics, Chem. Eng. Sci., **58**, 21 (2003), 4751–4768.
[17] A.N. Gorban, I.V. Karlin, and A.Y. Zinovyev, Constructive methods of invariant manifolds for kinetic problems, Phys. Reports, **396**, 4-6 (2004), 197–403.
[18] H. Struchtrup, Macroscopic transport equations for rarefied gas flows approximation methods in kinetic theory, Interaction of mechanics and mathematics series, Springer, Heidelberg, 2005
[19] A.N. Gorban and I.V. Karlin, Invariant manifolds for physical and chemical kinetics, Lect. Notes Phys. 660, Springer, Berlin, Heidelberg, 2005.
[20] I.V. Karlin, A.N. Gorban, Hydrodynamics from Grad's equations: What can we learn from exact solutions?, Ann. Phys. (Leipzig) **11** (2002), 783–833.

Dynamics of steps along a phase boundary

Anna Vainchtein
(joint work with Yubao Zhen)

Materials undergoing martensitic phase transitions are known to exhibit dissipative behavior due to the motion of phase boundaries. Classical nonlinear elasticity provides no information about kinetics of a phase boundary due to the inherent inability of the theory to describe phenomena in a narrow transition front where the energy dissipation occurs. This deficiency of the continuum theory motivated the recent studies of the dynamics of phase transitions in one-dimensional bistable chains where a kinetic relation between the driving force on a moving phase boundary and its velocity was derived from the discrete model [3, 4].

In this work we consider a phase boundary moving in a three-dimensional cubic lattice. In this setting it is important that a martensitic phase boundary typically contains *steps*, or ledges. A long-standing hypothesis in materials science is that a phase boundary moves forward via a propagation of steps *along* the interface [2]. This hypothesis is confirmed by experimental observations: for example, Bray and Howe [1] found the fcc/hcp martensite transformation in Co-Ni occurs by the passage of Shockley partial dislocation ledges and that the hcp martensite thickens by the lateral movement of ledges across the fcc/hcp interface. Thus kinetics of a phase boundary is largely determined by the kinetics of the steps. This work focuses on the dynamics of multiple steps along a phase boundary.

To enable analytical calculations, we assume antiplane shear deformation and consider a phase transforming material with a stress-strain law that is piecewise

linear with respect to one component of shear strain and linear with respect to another. Under these assumptions we derive a semi-analytical solution describing a steady sequential motion of the steps under an external loading. Our analysis yields kinetic relations between the driving force, the velocity of the steps and other characteristic parameters of the motion. These are studied in detail for the one-step, two-step and three-step configurations. We show that the kinetic relations are significantly affected by the material anisotropy. Our results indicate the existence of multiple solutions exhibiting sequential step motion.

We also conduct a series of numerical simulations to investigate stability of these solutions and study other phenomena associated with step nucleation. We show that sequential propagation of sufficiently small number of steps can be stable, provided that the velocity of the steps is below a certain critical value that depends on the material parameters and the step configuration. Above this value we observe a cascade nucleation of multiple steps which then join sequentially moving groups. Depending on material anisotropy, the critical velocity can be either subsonic or supersonic, resulting in subsonic step nucleation in the first case and steady supersonic sequential motion in the second. The numerical simulations are facilitated with an exact non-reflecting boundary condition and a fast algorithm for its implementation, which are developed to eliminate the possible artificial wave reflection from the computational domain boundary.

The details of this work can be found in [5, 6].

References

[1] D. Bray, J. Howe, *High-resolution transmission electron microscopy investigation of the face-centered cubic/hexagonal close-packed martensite transformation in Co-31.8 Wt Pct Ni alloy: Part I. Plate interfaces and growth ledges*, Metall. Mat. Trans. A **27A** (1996), 3362–3370.

[2] J. Hirth, *Ledges and dislocations in phase transformations*, Metall. Mat. Trans. A **25A** (1994), 1885–1894.

[3] L. I. Slepyan, A. Cherkaev, E. Cherkaev, *Transition waves in bistable structures. II. Analytical solution: wave speed and energy dissipation*, J. Mech. Phys. Solids, **53** (2005), 407–436.

[4] L. Truskinovsky, A. Vainchtein, *Kinetics of martensitic phase transitions: Lattice model*, SIAM J. Appl. Math. **66** (2005), 533–553.

[5] Y. Zhen, A. Vainchtein, *Dynamics of steps along a martensitic phase boundary I: Semi-analytical solution.*, J. Mech. Phys. Solids (2007), doi:10.1016/j-jmps.2007.05.017.

[6] Y. Zhen, A. Vainchtein, *Dynamics of steps along a martensitic phase boundary II: Numerical simulations.*, J. Mech. Phys. Solids (2007), doi:10.1016/j-jmps.2007.05.018.

Nonlinear electronic transport in the kinetic theory of semiconductor nanostructures

Luis L. Bonilla

Semiconductor superlattices (SL) are artificial one-dimensional (1D) crystals formed by repeating a number of periods comprising two layers of different semiconductors in the simplest case [1]. Applications include fast nanoscale oscillators,

quantum cascade lasers and infrared detectors. Ignoring scattering and electron-electron interaction, the Bloch theorem indicates that the Schrödinger equation for one electron in the 1D crystal potential has a continuum spectrum with minibands and minigaps and a basis whose wave functions are products of Bloch functions and plane waves in the directions perpendicular to the SL growth direction. We use this wave function basis to consider the effects of electron-electron interaction and electron-phonon scattering that are ignored in the one-electron picture [2]. Electronic transport in superlattices may be described by vector kinetic equations with as many components as minibands we want to consider. Quantum mechanics implies that the kinetic equations for the Wigner function contain pseudo-differential operators involving the electric potential and the miniband dispersion relations. Electron-phonon collisions can be modeled by nonlocal BGK (Bhatnagar-Gross-Krook) type terms involving collision-broadened Fermi-Dirac distributions. In the simplest case that only one miniband, the Wigner function $f(x,k,t)$ and the electric potential $W(x,t)$ solve the following system of equations:

$$(1)\qquad \begin{aligned}&\frac{\partial f}{\partial t}+\frac{i}{\hbar}\left[\mathcal{E}\left(k+\frac{1}{2i}\frac{\partial}{\partial x}\right)-\mathcal{E}\left(k-\frac{1}{2i}\frac{\partial}{\partial x}\right)\right]f\\&\quad+\frac{ie}{\hbar}\left[W\left(x+\frac{1}{2i}\frac{\partial}{\partial k},t\right)-W\left(x-\frac{1}{2i}\frac{\partial}{\partial k},t\right)\right]f\\&\quad=-\nu_{en}\left(f-f^{FD}\right)-\nu_{\mathrm{imp}}\frac{f(x,k,t)-f(x,-k,t)}{2},\end{aligned}$$

$$(2)\qquad \varepsilon\frac{\partial^2 W}{\partial x^2}=\frac{e}{l}\,(n-N_D),$$

$$(3)\qquad n=\frac{l}{2\pi}\int_{-\pi/l}^{\pi/l}f(x,k,t)dk=\frac{l}{2\pi}\int_{-\pi/l}^{\pi/l}f^{FD}(k;n)dk,$$

$$(4)\qquad f^{FD}(k;n)=\frac{m^*k_BT}{\pi\hbar^2}\int_{-\infty}^{\infty}\ln\left[1+\exp\left(\frac{\mu-E}{k_BT}\right)\right]\frac{\sqrt{2}\,\Gamma^3/\pi}{[E-\mathcal{E}(k)]^4+\Gamma^4}\,dE.$$

The Wigner function $f(x,k,t)$ is $2\pi/l$-periodic in k. Here n, N_D, $\mathcal{E}(k)$, d_B, d_W, $l=d_B+d_W$, ε, m^*, k_B, T, Γ, ν_{en}, ν_{imp} and $-e<0$ are the 2D electron density, the 2D doping density, the miniband dispersion relation (a typical one is $\mathcal{E}(k)=\Delta\,(1-\cos kl)/2$), the barrier width, the well width, the SL period, the SL permittivity, the effective mass of the electron, the Boltzmann constant, the lattice temperature, the energy broadening of the equilibrium distribution due to collisions, the frequency of the inelastic collisions responsible for energy relaxation, the frequency of the elastic impurity collisions and the electron charge, respectively.

Despite the complex appearance of these kinetic equations, their crystal periodicity makes it possible to derive balance equations for the electric field and the electron densities using singular perturbation methods. At high values of the electric field, the collision terms and the electric potential term in (1) are of the same order and dominate all others. In the resulting hyperbolic limit, the two first terms of the left hand side of (1) can be ignored and the resulting equation solved for the Fourier coefficients $f_j(x,t)$ of $f(x,k,t)=\sum_{j=-\infty}^{\infty}e^{ijkl}f_j(x,t)$ in terms of

the electron density and the electric field $-F$, $F = \partial W/\partial x$. This observation can be used to implement a Chapman-Enskog singular perturbation method that produces differential-difference spatially nonlocal balance equations for the electric field in a finite SL with N periods [2]:

$$(5)\ \varepsilon \frac{\partial F}{\partial t} + \mathcal{N}\left(F, \frac{\partial F}{\partial x}\right) = \left\langle D\left(F, \frac{\partial F}{\partial x}, \frac{\partial^2 F}{\partial x^2}\right)\right\rangle_1 + \left\langle A\left(F, \frac{\partial F}{\partial x}\right)\right\rangle_1 J(t).$$

In this Ampère equation for the balance of electric current, $J(t)$ is the total current density, $\langle g(x)\rangle_j = \int_{-jl/2}^{jl/2} g(x+s)\, ds/(jl)$ is a spatial average over j SL periods and the functions $\mathcal{N}$, D and A contain up to two spatial averages with $j = 1, 2$ [2]. Equation (5) is a nonlocal drift-diffusion equation for the unknowns $F(x,t)$ and $J(t)$ and it has to be supplemented by the dc voltage bias condition $\int_0^L F(x,t)\, dx = \Phi$, by boundary conditions at the intervals $(-2l, 0)$ and $(Nl, (N+2)l)$, with $L = Nl$, and by an initial condition $F(x, 0)$. When solved numerically, the resulting problem has stable time-periodic solutions that represent self-sustained oscillations of the current (for appropriate values of the voltage Φ) [2]. These high-frequency oscillations correspond to the periodic formation of a pulse of the electric field at the injecting contact of the superlattice, its motion towards the receiving contact and its annihilation there.

A detailed analysis of this type of solutions can be carried out in simplified piecewise linear *spatially local* drift-diffusion models [4] that mimic the current self-sustained oscillations described in the review [1]. In the toy model of Ref. [4], the drift velocity is a constant $K > 0$ and the source term has one stable and one unstable zero for a given value of the current J. For voltage bias, the current $J(t)$ varies slowly with time provided the sample length L is much larger than the size of the electric field pulse. For constant J, pulses are constructed as phase plane trajectories that join the stable zero $F = F^{(1)}(J)$, $\partial F/\partial\xi = 0$ ($\xi = x - X_\pm(t)$) with the pulse maximum $F = U(J)$, $\partial F/\partial\xi = 0$ and having either $\partial F/\partial\xi > 0$ for $-\infty < \xi < 0$ and $dX_+/dt = c_+$ or $\partial F/\partial\xi < 0$ for $0 < \xi < \infty$ and $dX_-/dt = c_-$. It is possible to prove that $c_+ + c_- = 2K$ and that $J(t)$ obeys a simple ordinary differential equation $dJ/dt = B(J)\,(c_+ - c_-)$ (with $B > 0$) when the pulse is far from the contacts at $x = 0$, $x = L$. Then provided it is far from the contacts, the pulse tends to a wave that moves rigidly with speed $c_+ = c_- = K$ until it arrives to the receiving contact. A more complicated analysis describes the annihilation of the pulse at $x = L$ and the nucleation of a new pulse at $x = 0$ when the current surpasses a critical value defined by the boundary condition at $x = 0$ [4].

Superlattices having two populated minibands or describing spin transport in the presence of spin-orbit interaction terms are described by vector kinetic equations for the Wigner matrix. It is possible to derive spatially nonlocal drift-diffusion systems of equation in these cases [3]. Self-sustained oscillations of the current at large dc voltages are typical solutions of the balance equations and they may describe spin oscillators in spintronic devices [5].

References

[1] L. L. Bonilla and H. T. Grahn, *Nonlinear dynamics of semiconductor superlattices*, Rep. Prog. Phys. **68** (2005), 577–683.

[2] L.L. Bonilla and R. Escobedo, *Wigner-Poisson and nonlocal drift-diffusion model equations for semiconductor superlattices*, Math. Mod. Meth. Appl. Sci. (M3AS) **15**(8) (2005), 1253–1272.

[3] L.L. Bonilla, L. Barletti and M. Alvaro, *Nonlinear electron and spin transport in semiconductor superlattices*. Preprint, 2007.

[4] L.L. Bonilla, M. Kindelan and J. B. Keller, *Periodically generated propagating pulses*, SIAM J. Appl. Math. **65** (2005), 1053–1079.

[5] L.L. Bonilla, R. Escobedo, M. Carretero and G. Platero, *Multiquantum well spin oscillator*, Appl. Phys. Lett. **91** (2007), 092102 (3 pages).

Structural phase transitions in perovskites

Paolo Cermelli

(joint work with Paolo Podio Guidugli)

We propose a simple mechanism to explain some features of the structural phase transitions characteristic of many ABO_3 perovskites. The relative stability of the cubic, rhombohedral and tetragonal phases is studied in terms of the competition between the equilibrium length and relative compressibility of the AO and BO bonds: adopting an empirical-potential description of interatomic forces, we assume that the AO bonds are approximately indeformable, and the O and B atoms interact through a "soft" Lennard-Jones potential. Since the equilibrium bond lengths have different thermal expansion coefficients, temperature variations generate an internal mismatch, measured by Goldschmidt's tolerance factor t, that is accommodated by the distortion of the perovskite structure responsible for the phase transitions. The distortion may be described in terms of the rotation vector of one of the AO_6 octahedra, and, neglecting electronic and magnetic effects, the interaction energy per cell may be written as a function of this vector order parameter. The stability analysis shows that, as t decreases, the cubic perovskite structure changes first to a rhombohedral and then to a tetragonal structure, as observed in many materials of this type. Our approach can be generalized to account for non-rigid deformations of the octahedra due to the Jahn-Teller effect in manganites.

Mechanical stresses in plant growth: from cells to veination networks

Arezki Boudaoud

(joint work with F. Corson, M. Adda-Bedia)

This talk is devoted to the mechanical aspects of plant growth and morphogenesis. The introductory part concerns the cellular level. The shape of a plant cell is sustained by its walls while it grows by plastic yielding to the inner osmotic

pressure. Consequently, a plant cell may be considered as a special pressure vessel: a viscoelastic or viscoplastic thin shell, pressurized from inside.

In our first contribution, we investigated the effect of mechanical stresses on growing stems, in connection with experiments (O. Hamant, Y. Couder and J. Traas) allowing the visualization in cells of microtubules (a stiff biopolymer). The mechanical model is again a pressure vessel, the shell standing for the outer layer of cells in the stem. By computing the stresses in the shell, we found that the microtubules align with the direction of largest principal stress. Thus biological microstructure is correlated with the state of mechanical stress.

In our second contribution, we investigated leaf venation networks which serve for fluid transport in grown leaves. These networks, like leaf shapes, are extremely diverse, yet their local structure satisfies a simple, universal property: the angles veins form at junctions are related to their diameters by a vectorial equation analogous to a force balance. This structure is the signature of a reorganization of vein networks during the development of leaves, a process we investigated numerically using a cell proliferation model. Provided that vein cells are given different mechanical properties, tensile forces develop along the veins during growth, causing the network to deform progressively. The statistics of the patterns obtained in these simulations are in quantitative agreement with observations on leaves, supporting the notion that the local structure of leaf venation networks reflects a balance of mechanical forces.

Buckling made easy

Yury Grabovsky
(joint work with Lev Truskinovsky)

It is commonly understood that buckling occurs whenever a compressive loading is applied to a slender body. But, what *exactly* is a "slender body" and compressive loading? In this regard it is instructive to mention D'Alembert's objection [5, p. 258] to Euler's analysis of buckling [1]. D'Alembert pointed out that if one applies a compressive dead load to a vertical column, the column would become unstable *immediately* due to flip instability[1]. In fact, D'Alembert's argument is valid even if the column is not slender at all. In buckling, the proper notion of slenderness involves not only the geometry of the body but also the degree of "softness of device". Indeed, it is well-known that Euler buckling never happens in hard device. Korn's constant provides just such a quantity, [4].

$$K(V) = \inf_{\substack{\boldsymbol{\varphi}\in V \\ \|\nabla\boldsymbol{\varphi}\|=1}} \int_\Omega |e(\boldsymbol{\varphi})|^2 d\boldsymbol{x}, \qquad e(\boldsymbol{\varphi}) = (\nabla\boldsymbol{\varphi} + (\nabla\boldsymbol{\varphi})^t)/2,$$

where V is a subspace of $W^{1,2}(\Omega;\mathbb{R}^2)$ and $\|\cdot\|$ always denotes the L^2-norm. In the purely soft device the Korn constant is zero (hence flip instability), while in the

[1]Euler himself have been careful to say that the column has "to be so constituted that it can not slip", [1, pp. 102-103].

purely hard device it is $1/2$, validating linear elasticity and preventing instability at small loads.

In order to understand properly the role of Korn's constant and formulate the notion of compressiveness, we formulate a model involving two small parameters h and λ, where $h > 0$ will govern the slenderness of the domain, while $\lambda < 0$ describes a compressive loading program.

$$\mathcal{E}(\boldsymbol{y}) = \int_{\Omega_h} W(\nabla \boldsymbol{y}) d\boldsymbol{x} - \int_{\partial\Omega_h} (\boldsymbol{t}_h(\boldsymbol{x};\lambda), \boldsymbol{u}) ds(\boldsymbol{x}), \tag{1}$$
$$\boldsymbol{y} \in \overline{\boldsymbol{y}}_h(\boldsymbol{x};\lambda) + V_h^0, \qquad V^0 \subset W^{1,\infty}(\Omega;\mathbb{R}^2).$$

The first formula above gives the energy of the deformation $\boldsymbol{y}$ as a sum of the elastic energy stored in the deformed body, whose reference configuration is Ω_h, and the work of the boundary tractions $\boldsymbol{t}_h(\boldsymbol{x};\lambda)$. The second formula gives boundary conditions in a general form that can accommodate a wide variety of mixed device loadings. The closer the space $V_h = \overline{V_h^0}$ to $W^{1,2}$, the closer we are to the soft device. The closer the space V_h to $W_0^{1,2}$, the closer we are to the hard device.

The energy density function $W(\boldsymbol{F})$ is assumed to be frame-indifferent, i.e. satisfy $W(\boldsymbol{RF}) = W(\boldsymbol{F})$ for every rotation $\boldsymbol{R}$ and every $\boldsymbol{F}$. We also assume that $\boldsymbol{F} = \boldsymbol{I}$ is the stress-free state, i.e. $W_{\boldsymbol{F}}(\boldsymbol{I}) = \boldsymbol{0}$. These two properties are responsible for both buckling and flip instability. The frame-indifference implies that there exists a function $\hat{W}(\boldsymbol{C})$ such that $W(\boldsymbol{F}) = \hat{W}(\boldsymbol{F}^t\boldsymbol{F})$. Let $\mathsf{L}(\boldsymbol{F}) = W_{\boldsymbol{FF}}(\boldsymbol{F})$. Then

$$(\mathsf{L}(\boldsymbol{F})\boldsymbol{\xi},\boldsymbol{\xi}) = 2(\hat{W}_{\boldsymbol{C}}(\boldsymbol{C}), \boldsymbol{\xi}^t\boldsymbol{\xi}) + 4(\hat{W}_{\boldsymbol{CC}}(\boldsymbol{C})(\boldsymbol{F}^t\boldsymbol{\xi}), \boldsymbol{F}^t\boldsymbol{\xi}). \tag{2}$$

In two dimensions, if $\boldsymbol{F} \approx \boldsymbol{I}$ and $\boldsymbol{\xi} = \boldsymbol{S} = \begin{bmatrix} 0 & -1 \\ 1 & 0 \end{bmatrix}$, then

$$(\mathsf{L}(\boldsymbol{F})\boldsymbol{S},\boldsymbol{S}) = \operatorname{Tr}(\mathsf{L}_0(\boldsymbol{F}-\boldsymbol{I})) + O(|\boldsymbol{F}-\boldsymbol{I}|^2), \qquad \mathsf{L}_0 = \mathsf{L}(\boldsymbol{I}) = W_{\boldsymbol{FF}}(\boldsymbol{I}).$$

We see that when $\boldsymbol{F} \approx \boldsymbol{I}$ the first term on the right-hand side in (2), corresponding to the incremental work of the prestress, dominates and the energy is non-convex at those $\boldsymbol{F} \approx \boldsymbol{I}$ for which $\operatorname{Tr}(\mathsf{L}_0(\boldsymbol{F}-\boldsymbol{I})) < 0$ (compressive loading), [3].

Our analysis of buckling instability is basically the above calculation applied to the study of non-negativity of second variation for the trivial branch, whose existence we postulate. More precisely, we assume the existence of a family of stationary points $\boldsymbol{y}_{h,\lambda}(\boldsymbol{x})$ of (1) satisfying

$$\boldsymbol{F}_{h,\lambda}(\boldsymbol{x}) = \nabla \boldsymbol{y}_{h,\lambda}(\boldsymbol{x}) = \boldsymbol{I} + \lambda \nabla \boldsymbol{u}_h'(\boldsymbol{x}) + o(\lambda),$$

where $\boldsymbol{u}_h'(\boldsymbol{x})$ solves

$$\int_{\Omega_h} (\mathsf{L}_0 e(\boldsymbol{u}_h'), e(\boldsymbol{\varphi})) d\boldsymbol{x} - \int_{\partial\Omega_h} (\boldsymbol{t}_h^{\mathrm{lin}}, \boldsymbol{\varphi}) ds = 0,\ \boldsymbol{u}_h' \in \overline{\boldsymbol{u}}_h + V_h^0,\ \overline{\boldsymbol{u}}_h = \frac{\partial \overline{\boldsymbol{y}}_h}{\partial \lambda}(\boldsymbol{x};0) \tag{3}$$

for all $\boldsymbol{\varphi} \in V_h = \overline{V_h^0}$, where $\boldsymbol{t}_h(\boldsymbol{x};\lambda) = \lambda \boldsymbol{t}_h^{\mathrm{lin}}(\boldsymbol{x}) + o(\lambda)$.

The function

$$m(h,\lambda) = \inf_{\substack{\boldsymbol{\varphi}\in V_h \\ \|\nabla\boldsymbol{\varphi}\|=1}} \delta^2\mathcal{E}(\boldsymbol{F}_{h,\lambda},\boldsymbol{\varphi}),\ \delta^2\mathcal{E}(\boldsymbol{F}_{h,\lambda},\boldsymbol{\varphi}) = \int_{\Omega_h} (\mathsf{L}(\boldsymbol{F}_{h,\lambda}(\boldsymbol{x}))\nabla\boldsymbol{\varphi}(\boldsymbol{x}), \nabla\boldsymbol{\varphi}(\boldsymbol{x})) d\boldsymbol{x}$$

describes the stability locus $\mathfrak{S} = \{(h,\lambda) \in (0,+\infty)\times(-\infty,0)\colon m(h,\lambda) \geq 0\}$ of the trivial branch in the (h,λ) parametric plane. We define a critical load as

$$\lambda(h) = \sup\{\lambda < 0\colon m(h,\lambda) < 0\}.$$

Definition: An instability of the trivial branch is called a *near-flip buckling* if

- $\lambda(h) < 0$ for sufficiently small h and
- $\lim_{h\to 0} \lambda(h) = 0$

The significance of the Korn constant is then immediately seen from the relation

$$\lim_{\lambda\to 0} m(h,\lambda) = \inf_{\substack{\boldsymbol{\varphi}\in V_h \\ \|\nabla\boldsymbol{\varphi}\|=1}} \int_{\Omega_h} (\mathsf{L}_0 e(\boldsymbol{\varphi}), e(\boldsymbol{\varphi}))d\boldsymbol{x} \stackrel{\text{def}}{=} K_{\mathsf{L}_0}(V_h).$$

We see that $K_{\mathsf{L}_0}(V_h) > 0$ is sufficient for $\lambda(h) < 0$, while $K_{\mathsf{L}_0}(V_h) \to 0$, as $h \to 0$ is necessary for $\lambda(h) \to 0$.

When h and λ are small we may replace the second variation $\delta^2\mathcal{E}(\boldsymbol{F}_{h,\lambda}, \boldsymbol{\varphi})$ with a simpler expression involving only the solution $\boldsymbol{u}'_h$ of the linearized elasticity equations (3). The key point is that the minimizer $\boldsymbol{\varphi}_{h,\lambda}$ (or almost minimizer, if the minimizer does not exist) must have a small (in L^2 sense) symmetrized gradient $e(\boldsymbol{\varphi}_{h,\lambda})$. Therefore, applying the formula (2) to the second variation and using the smallness of $e(\boldsymbol{\varphi}_{h,\lambda})$, we obtain

$$\delta^2\mathcal{E}(\boldsymbol{F}_{h,\lambda}, \boldsymbol{\varphi}_{h,\lambda}) = \int_{\Omega_h} \{(\mathsf{L}_0 e(\boldsymbol{\varphi}_{h,\lambda}), e(\boldsymbol{\varphi}_{h,\lambda})) + \lambda(\boldsymbol{\sigma}'_h(\boldsymbol{x}), (\nabla\boldsymbol{\varphi}_{h,\lambda})^t\nabla\boldsymbol{\varphi}_{h,\lambda})\}d\boldsymbol{x} + o(\lambda),$$

where $\boldsymbol{\sigma}'_h = \boldsymbol{\sigma}'_h(\boldsymbol{x}) = \mathsf{L}_0 e(\boldsymbol{u}'_h)$. In two space dimension we may further simplify the asymptotics for $\delta^2\mathcal{E}(\boldsymbol{F}_{h,\lambda}, \boldsymbol{\varphi}_{h,\lambda})$

$$\delta^2\mathcal{E}(\boldsymbol{F}_{h,\lambda}, \boldsymbol{\varphi}_{h,\lambda}) = \int_{\Omega_h} \{(\mathsf{L}_0 e(\boldsymbol{\varphi}_{h,\lambda}), e(\boldsymbol{\varphi}_{h,\lambda})) + \lambda t_h(\boldsymbol{x})|\nabla\boldsymbol{\varphi}_{h,\lambda}|^2\}d\boldsymbol{x} + o(\lambda),$$

where $t_h(\boldsymbol{x}) = \operatorname{Tr}\boldsymbol{\sigma}'_h/2$. This analysis suggests that we may replace $m(h,\lambda)$ with

$$\hat{m}(h,\lambda) = \inf_{\substack{\boldsymbol{\varphi}\in V_h \\ \|\nabla\boldsymbol{\varphi}\|=1}} \int_{\Omega_h} \left\{(\mathsf{L}_0 e(\boldsymbol{\varphi}), e(\boldsymbol{\varphi})) + \lambda t_h(\boldsymbol{x})|\nabla\boldsymbol{\varphi}|^2\right\} d\boldsymbol{x}.$$

We now introduce a measure of compressiveness

$$\mathfrak{c} = \sup_{\substack{\|e(\boldsymbol{\varphi}_h)\|\to 0 \\ \|\nabla\boldsymbol{\varphi}_h\|=1}} \overline{\lim_{h\to 0}} \int_{\Omega_h} t_h(\boldsymbol{x})|\nabla\boldsymbol{\varphi}_h|^2 d\boldsymbol{x}.$$

Theorem 1 If

- $\mathfrak{c} > 0$
- $K_{\mathsf{L}_0}(V_h) > 0$
- $\lim_{h\to 0} K_{\mathsf{L}_0}(V_h) = 0$

then the trivial branch undergoes a near-flip buckling instability. In that case we have the following expression for the critical buckling load.

Theorem 2 Assume that assumptions of Theorem 1 hold and that additionally

- $\lambda \mapsto \hat{m}(h, \lambda)$ is differentiable near $\lambda = 0$
- $\partial \hat{m}(h, \lambda)/\partial \lambda$ is continuous at $(0, 0)$
- $\mathfrak{c} > 0$

Then

$$\lim_{h \to 0} \frac{\lambda(h)}{K_{\mathsf{L}_0}(V_h)} = -\frac{1}{\mathfrak{c}}. \tag{4}$$

For structures with multiple slender elements the partial derivative $\hat{m}_\lambda$ is never continuous at $(0, 0)$ and (4) does not hold. Yet, the constitutive linearization procedure is still valid. In other words the critical load $\hat{\lambda}(h)$ determined using $\hat{m}(h, \lambda)$ has the same asymptotics as the true critical load $\lambda(h)$, as $h \to 0$. For complete discussion see [2].

References

[1] L. Euler. *Methodus inveniendi lineas curvas maximi minimive proprietate gaudentes sive solutio problematis isoperimetrici latissimo sensu accepti, Additamentum I. De curvis elasticis.* Bousquet, Lausannae et Genevae, 1744. Opera Omnia, Ser. I, Vol. 24. English translation by Oldfather, W. A. and Ellis, C. A. and Brown, D. M. in Isis, 20(1), pp. 72-160, 1933.

[2] Y. Grabovsky and L. Truskinovsky. The flip side of buckling. *Cont. Mech. Thermodyn.*, 19(3-4):211–243, 2007.

[3] R. Hill. On the elasticity and stability of perfect crystals at finite strain. *Math. Proc. Cambridge Philos. Soc.*, 77:225–240, 1975.

[4] C. O. Horgan. Korn's inequalities and their applications in continuum mechanics. *SIAM Rev.*, 37(4):491–511, 1995.

[5] C. Truesdell and W. Noll. *The non-linear field theories of mechanics.* Springer-Verlag, Berlin, third edition, 2004.

Reporter: Alessandro Turco

Participants

Dr. Marino Arroyo
Universitat Politecnica de
Catalunya (UPC)
Jordi Girona 1-3
Edifici C1
E-08034 Barcelona

Prof. Dr. Victor Berdichevsky
Department of Mechanical Eng.
2100 Engineering Building
Wayne State University
5050 Anthony Wayne Drive
Detroit , MI 48202-3902
USA

Dr. Thomas Blesgen
Max-Planck-Institut für Mathematik
in den Naturwissenschaften
Inselstr. 22 - 26
04103 Leipzig

Prof. Dr. Luis L. Bonilla
Departamento de Matematicas
Campus de Leganes
Universidad CarlosIII de Madrid
Avda. de la Universidad 30
E-28911 Leganes Madrid

Dr. Arezki Boudaoud
Departement de physique
Ecole normale superieure
24, rue Lhomond
F-75231 Paris Cedex 05

Prof. Andrea Braides
Dipartimento di Matematica
Universita di Roma "Tor Vergata"
Via della Ricerca Scientif. 1
I-00133 Roma

Prof. Dr. Yann Brenier
Laboratoire J.-A. Dieudonne
Universite de Nice
Sophia Antipolis
Parc Valrose
F-06108 Nice Cedex 2

Prof. Dr. Ana Maria Carpio
Departamento de Matematica Aplicada
Universidad Complutense de Madrid
E-28040 Madrid

Prof. Dr. Paolo Cermelli
Dipartimento di Matematica
Universita degli Studi di Torino
Via Carlo Alberto, 10
I-10123 Torino

Pierluigi Cesana
SISSA
International School for Advanced
Studies
Via Beirut n. 2-4
I-34014 Trieste

Dr. Antonin Chambolle
Centre de Mathematiques Appliquees
Ecole Polytechnique
Plateau de Palaiseau
F-91128 Palaiseau Cedex

Prof. Dr. Pierre Collet
Centre de Physique Theorique
Ecole Polytechnique
Plateau de Palaiseau
F-91128 Palaiseau Cedex

Prof. Dr. Sergio Conti
FB Mathematik
Universität Duisburg-Essen
Lotharstr. 65
47057 Duisburg

Prof. Gianni Dal Maso
S.I.S.S.A.
Via Beirut 2 - 4
I-34014 Trieste

Prof. Dr. Antonio DeSimone
SISSA
International School for Advanced Studies
Via Beirut n. 2-4
I-34014 Trieste

Prof. Dr. Marcelo Epstein
Dept. of Mechanical Engineering
University of Calgary
2500 University Drive N.W.
Calgary , AB T2N 1N4
CANADA

Prof. Dr. Adriana Garroni
Dipartimento di Matematica
"Guido Castelnuovo"
Universita di Roma "La Sapienza"
Piazzale Aldo Moro, 2
I-00185 Roma

Prof. Dr. Sergey L. Gavrilyuk
Laboratoire de Modelisation en Mecanique et Thermodynamique
Universite Aix-Marseille III
Avenue Escadrille Normandie-N.
F-13397 Marseille Cedex 20

Prof. Dr. Dmitry Golovaty
Department of Mathematical Sciences
University of Akron
Akron , OH 44325-4002
USA

Prof. Dr. Alexander N. Gorban
Department of Mathematics
University of Leicester
University Road
GB-Leicester , LE1 7RH

Prof. Dr. Yuri Grabovsky
Department of Mathematics
Temple University
Philadelphia , PA 19122
USA

Luca Heltai
SISSA
International School for Advanced Studies
Via Beirut n. 2-4
I-34014 Trieste

Giuliana Indelicato
Dipartimento di Matematica
Universita degli Studi di Torino
Via Carlo Alberto, 10
I-10123 Torino

Prof. Dr. Richard D. James
Department of Aerospace Engineering and Mechanics
University of Minnesota
110 Union Street S. E.
Minneapolis , MN 55455
USA

Prof. Dr. Jean-Francois Joanny
Institut Curie
Section Research, UMR 168
11, rue Pierre et Marie Curie
F-75248 Paris Cedex 05

Prof. Dr. Stephan Luckhaus
Mathematisches Institut
Universität Leipzig
Johannisgasse 26
04103 Leipzig

Prof. Dr. Jean-Jacques Marigo
Universite Pierre et Marie Curie
Institut Jean le Rond d'Alembert
CNRS, Tour 55-65
4, Place Jussieu
F-75252 Paris Cedex 05

Prof. Dr. Ingo Müller
Inst. für Verfahrenstechnik
FG Thermodynamik
Techn. Universität Berlin
Fasanenstr. 90
10623 Berlin

Prof. Dr. Stefan Müller
Max-Planck-Institut für Mathematik
in den Naturwissenschaften
Inselstr. 22 - 26
04103 Leipzig

Prof. Dr. Michael Ortiz
Division of Engineering and
Applied Sciences; MS 104-44
California Institute of Technology
Pasadena , CA 91125
USA

Prof. Dr. David Quere
ESPCI
10, rue Vauquelin
F-75231 Paris Cedex 5

Prof. Dr. Alexander G. Ramm
Department of Mathematics
Kansas State University
Manhattan , KS 66506-2602
USA

Prof. Dr. Frank Redig
Mathematical Institute
University of Leiden
Niels Bohrweg 1
NL-2300 RA Leiden

Prof. Dr. Henning Struchtrup
Dept. of Mechanical Engineering
University of Victoria
P.O.Boc 3055 STN CSC
Victoria, BC V8W 3P6
CANADA

Prof. Dr. Pierre Suquet
Laboratoire de Mecanique et
d'Acoustique
31 chemin Joseph Aiguier
F-13402 Marseille Cedex 09

Carlos Triguero
Laboratoire de Mecanique des
Solides
UMR-CNRS 7649
Ecole Polytechnique
F-91128 Palaiseau Cedex

Prof. Dr. Lev Truskinovsky
Laboratoire de Mecanique des
Solides
UMR-CNRS 7649
Ecole Polytechnique
F-91128 Palaiseau Cedex

Alessandro Turco
SISSA
International School for Advanced
Studies
Via Beirut n. 2-4
I-34014 Trieste

Prof. Dr. Anna Vainchtein
Dept. of Mathematics
University of Pittsburgh
301 Thackery Hall
Pittsburgh , PA 15260
USA

Prof. Dr. Michael Zaiser
School of Engineering and Electronics
University of Edinburgh
King's Buildings
Mayfield Road
GB-Edinburgh EH9 3JL

Dr. Giovanni Zanzotto
Dipartimento di Metodi e Modelli
Matematici
Universita di Padova
Via Trieste, 63
I-35121 Padova